Entrainment to natural oscillations
via uncoupled central pattern generators

Y. Futakata   and   T. Iwasaki

Abstract—**Mechanical systems can often be controlled efficiently by exploiting a resonance. An optimal trajectory minimizing an energy cost function is found at (or near) a natural mode of oscillation. Motivated by this fact, we consider the natural entrainment problem: the design of nonlinear feedback controllers for linear mechanical systems to achieve a prescribed mode of natural oscillation for the closed-loop system. We adopt a set of distributed central pattern generators (CPGs) as the basic control architecture, inspired by biological observations. The method of multivariable harmonic balance (MHB) is employed to characterize the condition, approximately, for the closed-loop system to have a natural oscillation as its trajectory. Necessary and sufficient conditions for satisfaction of the MHB equation are derived in the forms useful for control design. It is shown that the essential design freedom can be captured by two parameters, and the design parameter plane can be partitioned into regions, in each of which approximate entrainment to one of the natural modes, with an error bound, is predicted by the MHB analysis. Control mechanisms underlying natural entrainment, as well as limitations and extensions of our results, are discussed.**

I. INTRODUCTION

During animal locomotion, periodic body movements generate propulsion through interactions with the surrounding environment. The associated energy consumption appears to be minimized by exploiting a mechanical resonance. For instance, the cycle period of human walking would be related to the natural frequency of the leg as a pendulum [1]. More generally, optimal controls of mechanical systems, to achieve a sustained periodic motion most efficiently, would often result in trajectories resembling a natural mode of oscillation. A fundamental question is how a feedback controller can be designed to achieve an oscillation at (or near) a natural mode as a stable limit cycle for the closed-loop system.

Rhythmic body movements (or "gaits") during animal locomotion are controlled by the neuronal circuit called the central pattern generator (CPG) [2]–[4]. CPGs are biological oscillators comprising a group of neurons interconnected in a specific manner to generate coordinated oscillations (or patterns) of neuronal membrane potentials. Placed in a feedback loop, a CPG activates rhythmic muscle contractions, where the commanded pattern is modified through sensory signals in response to changes in the environment and body mechanics. In this way, CPG integrates the trajectory planning with

Y. Futakata is with Department of Information Physics and Computing, The University of Tokyo, Tokyo, Japan, Yoshiaki_Futakata@ipc.i.u-tokyo.ac.jp. T. Iwasaki (corresponding author) is with Department of Mechanical and Aerospace Engineering, University of California, Los Angeles, CA 90095, tiwasaki@ucla.edu

feedback regulation, and provides a fundamental nonlinear control architecture for achieving adaptive pattern formation.

The architecture of CPGs is often given as coupled oscillators with distributed sensing and actuation. For undulatory swimming animals like leeches and lampreys, for instance, the CPG is formed as a chain of segmental oscillators, each of which receives local sensory feedback and induces local muscle contraction [5], [6]. The intersegmental communication was considered essential for coordinating the phase timing of the oscillators so that traveling body waves are generated. However, experiments have shown that, even if the nerve cord connecting the segmental oscillators is severed in the midbody, the leech can still swim by coordinating the head and tail undulations through local controls and mechanical linkages [7]. Thus, CPG-based control systems can be robust against failures. Moreover, the result suggests that decentralized controls by uncoupled oscillators can achieve coordination.

In this paper, we take a first step toward exploring the potential of CPGs as a basic control unit to achieve desired oscillations for mechanical systems. The long-term goal is to establish a CPG-based feedback control theory to generate efficient gaits for robotic locomotor systems. Such theory would enable development of biologically-inspired robotic systems that are robust against failures and adaptive to changes in the operating condition. Exploitation of a resonance, or natural oscillations, would have an obvious advantage for increased energy efficiency, but would also make the system conform to, rather than compete against, environmental constraints, leading for instance to swimming gaits that are least disturbing to the fluid. As a byproduct, such theory would contribute to advancing biological understanding of gait generation mechanisms in animal locomotion. To this end, this paper considers a *natural entrainment problem*, where we seek to design a controller comprising CPG units for mechanical systems so that the closed-loop system oscillates at (or near) a prescribed mode of natural oscillation.

For single degree-of-freedom (DOF) systems, the natural entrainment problem has been addressed in the literature [8]–[12] using harmonic balance (see e.g. [13], [14]). Harmonic balance is a well-known method for oscillation analysis that approximates periodic signals by sinusoids. The method is approximate in nature, but has been successfully applied to a variety of engineering problems [15]–[18]. References [8]–[12] used the harmonic balance to analyze the feedback connection of a one-DOF oscillatory mechanical system and a simple CPG called the reciprocal inhibition oscillator [19], [20]. The harmonic balance equation accurately predicted when the closed-loop oscillation had a frequency close to the resonance.

For multi-DOF systems, the natural entrainment problem has not been addressed. While the classical harmonic balance method has been used mostly for estimating the frequency and amplitude of a single variable oscillation, relative phases and amplitudes of multivariable oscillations are of paramount importance in characterizing coordinated rhythmic motion pattern. Recently, we have developed the method of multivariable harmonic balance (MHB) to analyze CPGs consisting of multiple identical neurons (with no connection to mechanical systems) [21]. A simple characterization of the oscillation profile (frequency, amplitudes, phases) was given in terms of the neuronal interconnection matrix. The MHB method, like the original harmonic balance, has no theoretical guarantee for accuracy of the predicted oscillation profile, but numerical simulations of various CPGs have shown that the predictions are reasonably accurate [21]–[23]. Moreover, it has also been shown [24] that the MHB method provides an exact estimate of the oscillation profile when the CPG has a certain structure.

The present paper extends the one-DOF result in [12] for multi-DOF linear mechanical systems. Motivated by the severed nerve cord experiment on leeches mentioned above, we consider distributed feedback controllers with multiple CPG units of the reciprocal inhibition oscillators. In particular, an n-DOF system with m pairs of sensors and actuators is driven by m CPG control units, each placed between a sensor/actuator pair. The CPGs are uncoupled to each other except for the indirect communication through the mechanical linkage with local sensory feedback. Unlike the single-DOF case, the natural entrainment problem involves matching of not only the frequency but also the mode shape. This additional complexity, together with the simple decentralized control structure, makes the problem substantially more difficult.

To gain insights into the natural entrainment mechanism, we will first focus on a class of systems motivated by biomechanics of animal body, where sensors, actuators, stiffness, and damping, are all collocated. A necessary and sufficient condition on the controller parameters is obtained for the MHB equation to have a solution at a given frequency and mode shape. It is shown that the essential design freedom is captured by two parameters: the intrinsic CPG frequency ω_o and the feedback gain η. The result allows us to draw a mode partition diagram, where the parameter plane (ω_o, η) is divided into regions, in each of which entrainment to a natural mode of oscillation is achieved approximately, with an explicit bound on the entrainment error. The assumption of collocation will then be removed and the results are extended for more general mechanical systems, with additional difficulties identified and discussed. A numerical example is given to illustrate the method and assess approximation errors inherent with the MHB method. Finally, we discuss what we have learned from our results regarding control mechanisms underlying natural entrainment. Limitations and possible extensions of our results are also discussed, where the controller designed by our method is proven to guarantee existence of Y-oscillations [25].

The MHB method is not perfectly accurate in general, but our developments are rigorous in the sense that all conditions are exactly derived from the MHB equation with no approximations. While lemmas and theorems are precisely stated, we choose to make less accurate but more insightful statements in the texts for brevity. For instance, we say "the controller achieves natural entrainment" when we mean "the MHB equation for the given controller has a natural oscillation as a stable solution." All statements become accurate if interpreted within the MHB framework. Some preliminary lemmas and all proofs are given in the Appendix. A conference version of this paper has appeared in [26], where some results for collocated systems were reported without proofs.

We use the following notation. Let $\jmath := \sqrt{-1}$. For complex matrices A and B, $A \otimes B$ denotes the Kronecker product, $B^\dagger$ is the Moore-Penrose inverse, and $\Im(A)$ is the imaginary part of A. When A is real symmetric, $A > 0$ and $A \geq 0$ mean that it is positive definite and positive semidefinite, respectively. The symbols $\mathbb{R}_+$ and $\mathbb{I}_n$ denote the set of real positive numbers and the set of integers from 1 to n, respectively. For a vector $v \in \mathbb{R}^n$ with the ith entry v_i, the $n \times n$ diagonal matrix whose (i,i) entry is v_i is denoted by $\mathrm{diag}(v)$ or $\mathrm{diag}(v_1, \ldots, v_n)$. For two sets $\mathbb{F}_1$ and $\mathbb{F}_2$ sharing the same underlying space, $\mathbb{F}_1 \backslash \mathbb{F}_2$ is the set of elements in $\mathbb{F}_1$ that do not belong to $\mathbb{F}_2$.

II. PROBLEM FORMULATION AND APPROACH

A. Natural Entrainment Problem

Consider the class of mechanical systems given by

$$J\ddot{x} + D\dot{x} + Kx = Bu, \quad y = Cx, \qquad (1)$$

where $x(t) \in \mathbb{R}^n$, $u(t) \in \mathbb{R}^m$, and $y(t) \in \mathbb{R}^m$ are the generalized coordinates, inputs, and outputs, respectively, and the inertia, damping, and stiffness matrices are symmetric and satisfy $J > 0$, $D \geq 0$, and $K \geq 0$. Note that the number of inputs is assumed to be the same as the number of outputs. For later reference, let us recall that a natural mode of (1) is defined by a pair of the natural frequency $\omega_i \in \mathbb{R}_+$ and mode shape $\xi_i \in \mathbb{R}^n$ satisfying $(K - \omega_i^2 J)\xi_i = 0$ with $\xi_i \neq 0$. There are n natural modes, (ω_i, ξ_i) with $i \in \mathbb{I}_n$, for the n-DOF system. We assume that the natural frequencies are distinct, and arrange them in the ascending order: $0 \leq \omega_1 < \omega_2 < \cdots < \omega_n$. We will develop a design theory for the *linear* system (1), but as for any linear theory, our results are expected to be applicable to (weakly) nonlinear systems whose dynamics near a targeted oscillatory trajectory can be captured reasonably well by (1). A design example will illustrate this point later in Section V.

To entrain the mechanical system (1) we use the reciprocal inhibition oscillator as the basic control unit. The reciprocal inhibition oscillator is a simple CPG consisting of two neurons with mutually inhibitory synaptic connections as shown in Fig. 1, where $\mathcal{N}$ represents a neuron and $\mu > 0$ is the strength of the synaptic connections between the neurons. The neuronal dynamics $\mathcal{N}$ is modeled by the following mapping from the synaptic input w to the membrane potential at axon (or spike frequency) v [12]:

$$v = \psi(\mathrm{q}), \quad \mathrm{q} = b(s)w, \quad b(s) := \frac{2\omega_o s}{(s + \omega_o)^2},$$

where q is an internal variable (e.g. membrane potential at soma), and $\omega_o > 0$. We choose the band pass filter $b(s)$ to embed the time lag and adaptation effects of the cell membrane

and synapse. A typical simple model for neuronal dynamics would capture the time lag effect by a low pass filter [27], but the adaptation (high pass) effect is also included here because it is essential for a reciprocal inhibition oscillator [20]. The static nonlinearity $\psi : \mathbb{R} \to \mathbb{R}$ captures the threshold and saturation effects; it is typically a sigmoid function and the following properties are assumed:

- ψ is odd, bounded, and strictly increasing.
- $\psi(x)$ is strictly concave on $x > 0$, and $\psi'(0) = 1$.

We denote by Ψ the class of functions satisfying these conditions. For example, $\tanh(x)$ belongs to this class.
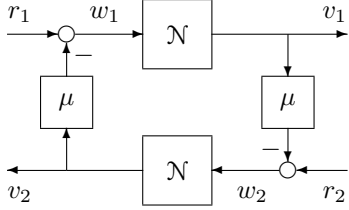

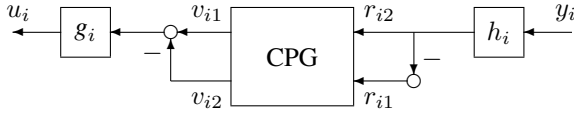Fig. 1.   Reciprocal inhibition oscillator CPG

Fig. 2.   CPG control unit

Following the development in [12], we place the control unit in Fig. 2 for each input/output pair (u_i, y_i) of the mechanical system, where g_i and h_i are feedback gains and the block labeled as "CPG" represents the system in Fig. 1. This architecture is motivated by the biological control mechanism where the neurons in the CPG receive sensory feedback [28], and the membrane potentials of the neurons are used for muscle activation [29].

The CPGs share the same center frequency ω_o in the band pass filter and synaptic strength μ. Let $q_i(t) := [\, q_{i1} \quad q_{i2}\,]^\mathsf{T} \in \mathbb{R}^2$ be the internal variable for the ith CPG unit and define $q(t) \in \mathbb{R}^{2m}$ by stacking $q_i(t)$ in a column. The set of m units can be written as

$$q = b(s)\left(M\Psi(q) + Hy\right), \quad u = G\Psi(q) \tag{2}$$

where, with the $k \times k$ identity matrix denoted by I_k,

$$g := [g_1 \ \cdots \ g_n]^\mathsf{T}, \quad G := \mathrm{diag}(g) \otimes l^\mathsf{T}, \quad M := I_m \otimes M_o,$$
$$h := [h_1 \ \cdots \ h_n]^\mathsf{T}, \quad H := \mathrm{diag}(h) \otimes l, \quad l := [1 \ -1]^\mathsf{T},$$
$$M_o := -\mu \begin{bmatrix} 0 & 1 \\ 1 & 0 \end{bmatrix}, \quad \Psi := \psi I_{2m}.$$

Reference [12] has shown that, with $y(t) \equiv 0$ and $\mu > 1$, the internal variable q_i in the ith CPG autonomously oscillates, and q_{i1} and q_{i2} are antiphase to each other; $q_{i1}(t) = -q_{i2}(t)$. The harmonic balance method predicts the frequency of the autonomous oscillation to be the center frequency ω_o of $b(s)$. For this reason, ω_o is an approximated intrinsic frequency of the CPG, and we call it the CPG frequency. In the presence of arbitrary input y, the structure of H guarantees that the antiphase property of each CPG oscillation is preserved and

$$\lim_{t \to \infty} |q_{i1}(t) + q_{i2}(t)| = 0, \tag{3}$$

for any initial states $q_i(0)$ and $\dot{q}_i(0)$ [12].

The closed-loop system consisting of the mechanical system (1) and the CPG controller (2) is described by the kernel representation:

$$\mathcal{G}(s, \Psi)z = 0, \quad z := \begin{bmatrix} x \\ q \end{bmatrix}, \tag{4}$$

$$\mathcal{G}(s, \Psi) := \begin{bmatrix} Js^2 + Ds + K & -BG\Psi \\ b(s)HC & b(s)M\Psi - I \end{bmatrix}. \tag{5}$$

We consider the feedback control system in (4) and address the following problem.

> **Natural Entrainment Problem:** Characterize a domain of the controller parameter space in which entrainment to a prescribed mode of natural oscillation is achieved approximately, and obtain a bound on the entrainment error.

Formulation of the problem in the approximate setting is motivated by multiple factors; (a) allowing a small entrainment error is expected to substantially enlarge the feasible domain of controller parameter space as in the one-DOF case [12], providing more flexibility in the design, (b) a small entrainment error will not cause significant degradation in performance for practical purposes, and (c) exact analysis of limit cycles is extremely difficult for systems of dimension higher than two. We shall address the problem using an approximate method based on the idea of harmonic balance and describing functions. Numerical experiments will be used later in Section V to illustrate that our approximate results can be reasonably accurate. Throughout the paper, the mechanical system (1) and the static nonlinearity $\psi \in \Psi$ in the CPGs are assumed to be given.

B. Multivariable Harmonic Balance

To characterize an oscillation profile of the closed-loop system (4), assume that (4) has a periodic solution $z(t)$ with frequency ω. We shall approximate $z(t)$ by sinusoidal signals. In this case, we have

$$x_i(t) \cong r_i \sin(\omega t + \varphi_i), \tag{6}$$

$$q_i(t) \cong \begin{bmatrix} a_i \sin(\omega t + \phi_i) \\ -a_i \sin(\omega t + \phi_i) \end{bmatrix}, \tag{7}$$

for some amplitudes $r_i, a_i > 0$, and phase parameters $\varphi_i, \phi_i \in \mathbb{R}$, where $i \in \mathbb{I}_n$ in (6), and $i \in \mathbb{I}_m$ in (7), and the two signals in $q_i(t)$ are antiphase due to (3), and all signals oscillate with zero bias (the average over a cycle is zero) because the static gain of the neuronal dynamics is zero ($b(0) = 0$) and ψ is an odd function. Let $\hat{z} \in \mathbb{C}^{n+2m}$ be the phasor of $z(t)$:

$$\hat{z} = \begin{bmatrix} \hat{x} \\ \hat{q} \end{bmatrix}, \quad \begin{aligned} \hat{x}_i &:= r_i e^{\jmath\varphi_i}, \\ \hat{q}_i &:= \hat{\alpha}_i l, \quad \hat{\alpha}_i := a_i e^{\jmath\phi_i}, \end{aligned}$$

where $\hat{x} \in \mathbb{C}^n$ and $\hat{q} \in \mathbb{C}^{2m}$ are the vectors specified by their i^{th} entries $\hat{x}_i \in \mathbb{C}$ and $\hat{q}_i \in \mathbb{C}^2$, respectively. Similarly, we define $\hat{\alpha} \in \mathbb{C}^m$ by stacking $\hat{\alpha}_i$ in a column, which contains

all the information for $\hat{q}$. When the input is a sinusoid, the nonlinearity ψ may be approximated by

$$\psi(z) \cong \kappa(a)z \quad \text{for} \quad z := a\sin\omega t,$$
$$\kappa(a) := \frac{4}{a\pi}\int_0^{\pi/2}\psi(a\sin\theta)\sin\theta\,d\theta,$$

where $\kappa(a)$ is called the describing function [14], representing the effect of the static nonlinearity ψ by the amplitude-dependent linear gain $\kappa(a)$. It was shown in [12] that $\kappa(a)$ for $\psi \in \Psi$ takes a value in the interval $(0, 1)$ when $a > 0$, and κ is strictly decreasing from 1 to 0 on $a > 0$.

For a set of fixed amplitudes a_i of q_i-oscillations, the nonlinear function $\psi I(q_i)$ may be approximated by the describing function $\kappa(a_i)q_i$. In this case, the CPG control unit in Fig. 2 is quasi-linearized to have the transfer function $r_i(s)$ from y_i to u_i, where

$$r_i(s) := 2g_i\kappa_i p_i(s/\omega_o), \quad \kappa_i := \kappa(a_i),$$
$$p_i(s) := \frac{2h_i s}{s^2 + 2(1 - \mu\kappa_i)s + 1}. \tag{8}$$

Note that $p_i(s/\omega_o)l$ is the transfer function from y_i to q_i. Accordingly, the closed-loop system (4) is also quasi-linearized and is described by

$$\mathcal{G}(s, \Phi)z = 0, \quad \Phi := \text{diag}(\kappa_1, \cdots, \kappa_m) \otimes I,$$

where Φ is an amplitude-dependent matrix gain that approximates the nonlinear function Ψ for sinusoidal inputs. If the closed-loop system (4) has a periodic solution z that can be approximated by sinusoids as in (6) and (7), then the signals may be estimated by harmonic solutions to the quasi-linear system. Such solutions can be found by solving

$$\mathcal{G}(\jmath\omega, \Phi)\hat{z} = 0$$

for $(\omega, \hat{z})$. This is what we call the multivariable harmonic balance (MHB) equation.

We have found that an alternative description of the quasi-linear system is more directly useful for our analysis. Eliminating q from $\mathcal{G}(s, \Phi)z = 0$ and finding an equation for x, we obtain an equivalent quasi-linear system

$$A(s)x = 0, \quad A(s) := Js^2 + Ds + K - BR(s)C,$$
$$R(s) := \text{diag}(r(s)). \tag{9}$$

Similarly, the MHB equation reduces to

$$A(\jmath\omega)\hat{x} = 0, \quad \hat{\alpha}_i = p_i(j\omega/\omega_o)\hat{y}_i, \quad \kappa_i := \kappa(|\hat{\alpha}_i|) \tag{10}$$

where $\hat{y}_i$ is the ith entry of $\hat{y} := C\hat{x}$.

The basic idea of the MHB method [21] is the following.

- If the MHB equation (10) has a solution $(\omega, \hat{x}, \hat{\alpha})$, then the system (4) is expected to possess an oscillatory trajectory, approximately given by $x_i(t) \cong \Im[\hat{x}_i e^{\jmath\omega t}]$ and $q_i(t) \cong \Im[\hat{\alpha}_i e^{\jmath\omega t}]l$, or equivalently, (6) and (7).
- The estimated oscillation $(\omega, \hat{x}, \hat{\alpha})$ is expected to be stable if the associated quasi-linear system (9), defined for the amplitudes $a_i := |\hat{\alpha}_i|$, is marginally stable, with a pair of poles $\pm\jmath\omega$ on the imaginary axis and the rest in the open left half plane.[1]

---

[1] We shall refer to this property *the* marginal stability condition, which is stronger than the usual notion of marginal stability in that multiple pairs of nonrepeated poles are not allowed on the imaginary axis.

For given values of mechanical parameters (J, D, K, B, C) and controller parameters (ω_o, μ, g, h), the profile of closed-loop oscillations can be estimated as (6) and (7) by solving the MHB condition (10) for $(\omega, \hat{x}, \hat{\alpha})$. Note that $A(\jmath\omega)$ depends on $\hat{\alpha}_i$ through κ_i, and this makes it nontrivial to solve the MHB condition. The solution is not unique in general, and the MHB method may predict existence of multiple oscillations for the closed-loop system. The marginal stability of the associated quasi-linear system helps to identify the stable oscillation(s) among those predicted. The idea behind this heuristics can be found in [13], and is discussed further in Section VI. We shall call $(\omega, \hat{x}, \hat{\alpha})$ a *stable solution* of the MHB equation if it satisfies (10) and the associated quasi-linear system (9) satisfies the marginal stability condition as described above.

In the developments below, the phasor $\hat{\alpha}$ is possibly complex, and all the other parameters are real, with ω, ω_o, and μ being positive. In particular, phasors $\hat{x}$ and $\hat{y}$ will be real vectors since the mode shapes ξ_ℓ for $\ell \in \mathbb{I}_n$, that we aim to achieve (i.e., $\hat{x} = \xi_\ell$) by feedback control, are real vectors. This means that every variables $x_i(t)$ oscillate inphase or antiphase to each other, which is a property typical to natural oscillations of mechanical systems without interactions with the environment. The phasor $\hat{\alpha}_i$ would be complex with nonzero imaginary part when $\alpha_i(t)$ oscillates with a phase that is not a multiple of π with respect to $x_i(t)$. We shall avoid trivial cases by restricting our attention to oscillations such that $\hat{y}_i\hat{\alpha}_i \neq 0$ for all $i \in \mathbb{I}_m$. That is, we consider the nontrivial cases where every CPG unit receives a nonzero input and oscillates. The CPG control unit in Fig. 2 has the symmetry such that the dynamical mapping from y_i to u_i for (g_i, h_i) is the same as that for $(-g_i, -h_i)$. For instance, two units for $(g_i, h_i) = (3, -5)$ and $(-3, 5)$ have an identical input/output property. Thus, the sign of g_i is not important and can be chosen arbitrarily by adjusting the sign of h_i, or vice versa. In our results presented later, we have taken the sign of h_i to be the same as the sign of $\hat{y}_i$.

III. NATURAL ENTRAINMENT OF COLLOCATED MECHANICAL SYSTEMS

In this section, we consider a special class of mechanical systems (1) to gain analytical insights into mechanisms underlying natural entrainment. We will later discuss an extension of our results to a more general class of systems. To this end, let us introduce the following:

Assumption 1: The matrices B and C are square nonsingular ($m = n$), and

$$C = B^\mathsf{T}, \quad D = \rho K, \quad K = B\mathcal{K}C, \quad \mathcal{K} := \text{diag}(k_1, \cdots, k_m)$$

for positive scalars ρ and k_i with $i \in \mathbb{I}_m$.

The conditions in Assumption 1 are motivated by biological systems where the actuators, sensors, stiffness and damping elements are all located at the same position. A musculo-skeletal body can be viewed as a set of multiple rigid links connected by rotational joints. At each joint, the muscle and tendon serve as the origin of visco-elastic property, in addition to taking the role of torque actuator. Moreover, the muscle length, directly related to the joint angle, is fed

back to the motor control system through stretch receptors. Thus, the collocation arises naturally in biomechanics. In this case, the stiffness and damping matrices K and D share the same structure; a diagonal matrix sandwiched by the actuation matrix B and its transpose. This fact can readily be verified through the principle of virtual work. The additional assumption of Rayleigh damping $D = \rho K$ is commonly used in structural dynamics, and is introduced so that the analysis becomes simple enough to provide insights into the natural entrainment mechanism. We shall refer to the system (1) satisfying Assumption 1 as the *collocated system*.

A. Difficulty in Exact Natural Entrainment

Consider the problem of designing a CPG controller that achieves entrainment to a natural mode of oscillation *exactly*, within the framework of the MHB method. That is, we seek conditions on the controller (2) such that the MHB equation (10) has a solution $(\omega, \hat{x}, \hat{\alpha})$ with $\omega = \omega_\ell$ and $\hat{x} = \xi_\ell$ for a prescribed mode $\ell \in \mathbb{I}_n$. It is straightforward to show [30] that the set of all such controllers is given by

$$\mu = \frac{1}{\kappa(a)}, \quad g_i = \frac{\zeta_\ell k_i \hat{y}_i}{a\kappa(a)}, \quad h_i = \frac{a\varpi}{\hat{y}_i},$$

where

$$\zeta_\ell := \frac{\rho\omega_\ell}{2}, \quad \varpi := \frac{1}{2}\left(\frac{\omega_o}{\omega_\ell} - \frac{\omega_\ell}{\omega_o}\right). \quad (11)$$

In this case, the phasor of q is specified from $\hat{\alpha}_i = -\jmath a$. The controller is parametrized by two arbitrary real positive scalars: the amplitude of q-oscillation a and the intrinsic RIO frequency ω_o. Thus we have a very simple parametrization of all controllers to achieve entrainment to the natural oscillation (ω_ℓ, ξ_ℓ).

However, the resulting oscillations are not always stable. When the above controller is used for entrainment to the lowest mode (ω_1, ξ_1) or to the highest mode (ω_n, ξ_n), the associated quasi-linear system (9) satisfies the marginal stability condition if and only if ω_o is chosen such that $\omega_o < \omega_1$ or $\omega_n < \omega_o$, respectively. On the other hand, the system (9) is unstable for any values of (a, ω_o) when $1 < \ell < n$. This means that the CPG controller (2), with any choice of the parameters, would not be able to achieve entrainment to an intermediate mode of natural oscillation for collocated systems of three or higher DOF. This negative prediction of the MHB analysis has been confirmed to be correct through numerical simulations of some example systems. These results can be found in [30] and are not reported here for brevity.

Given the limitation in precisely achieving a natural oscillation, we shall relax the control specification such that the desired frequency may not exactly coincide with, but is close to, a natural frequency, while a natural mode shape is exactly enforced. Thus, in the sections that follow, we consider the control design to achieve entrainment to (ω, ξ_ℓ) with $\omega \cong \omega_\ell$. It turns out that this relaxation reveals a certain robustness property of the natural entrainment as in the case of one-DOF systems [12]. In particular, we will show that a large region of a controller parameter space leads to approximate natural entrainment to (ω, ξ_ℓ) with a bound on the error $|\omega - \omega_\ell|$.

Moreover, the parameter space, if chosen appropriately, can be partitioned into multiple regions, in each of which approximate entrainment to (ω_ℓ, ξ_ℓ) or (ω_o, ξ_ℓ) with $\ell \in \mathbb{I}_n$ is achieved. To this end, we shall first identify the essential parameter space in the next section.

B. Essential Parameters for Control Design

Let us first write down a necessary and sufficient condition for an oscillation profile $(\omega, \hat{x}, \hat{\alpha})$ with $\hat{x} := \xi_\ell$ to be a solution to the MHB equation (10). Exploiting the collocation structure of the mechanical system (1) as described in Assumption 1, the MHB condition can be decomposed into m scalar equations for harmonic balance of each input/output channel.

Lemma 1: Let the mechanical system (1), controller (2), and an oscillation profile $(\omega, \hat{x}, \hat{\alpha})$ be given. Suppose Assumption 1 holds, $\hat{x} = \xi_\ell$ for some $\ell \in \mathbb{I}_n$, and $h_i\hat{y}_i \neq 0$ for all $i \in \mathbb{I}_m$, where $\hat{y} := C\hat{x}$. Then the MHB equation (10) is satisfied if and only if

$$\mathfrak{f}_\ell(\omega) = 1 - \mu\kappa(|\hat{\alpha}_i|), \quad \mathfrak{g}_\ell(\omega) = \frac{g_i h_i}{\mu k_i}, \quad \mathfrak{h}_\ell(\omega) = \frac{h_i \hat{y}_i}{\hat{\alpha}_i}, \quad (12)$$

hold for all $i \in \mathbb{I}_m$, where

$$\varpi_o := \frac{1}{2}\left(\frac{\omega}{\omega_o} - \frac{\omega_o}{\omega}\right), \quad \varpi_\ell := \frac{1}{2}\left(\frac{\omega}{\omega_\ell} - \frac{\omega_\ell}{\omega}\right), \quad (13)$$

$$\mathfrak{f}_\ell(\omega) := \frac{\varpi_o \varpi_\ell}{\zeta_\ell}, \quad \mathfrak{g}_\ell(\omega) := \frac{\omega\varpi_o(\varpi_\ell^2 + \zeta_\ell^2)}{\omega_\ell(\varpi_o\varpi_\ell - \zeta_\ell)},$$
$$\mathfrak{h}_\ell(\omega) := \varpi_o\left(\frac{\varpi_\ell}{\zeta_\ell} + \jmath\right). \quad (14)$$

Recall that there are $2m + 2$ real scalar parameters for the controller; μ, ω_o, g_i, and h_i for $i \in \mathbb{I}_m$. By requiring that the MHB equation have a solution $(\omega, \xi_\ell, \hat{\alpha})$, the freedom in the choice of the controller parameters substantially reduces. In particular, condition (12) implies that the *uniformity and proportionality conditions* must be satisfied, i.e., (i) the amplitudes of the sensory feedback, $h_i\hat{y}_i$, are uniform over all CPG units (or $i \in \mathbb{I}_m$), and (ii) the overall feedback gain, g_ih_i, is proportional to the stiffness of the input/output channel k_i. Based on these observations, let us introduce a normalized feedback gain $\eta := (g_ih_i)/(\mu k_i)$. Once three parameters ω_o, η, and μ are specified, the rest of the parameters in the controller (g, h) as well as oscillation profile $(\omega, \hat{\alpha})$ can be determined by solving (12). This process is summarized as follows.

Procedure 1:

1. Let a desired mode of oscillation ℓ and the controller parameters ω_o, η, and μ be given.
2. Solve $\mathfrak{g}_\ell(\omega) = \eta$ for $\omega > 0$.
3. Solve $\mathfrak{f}_\ell(\omega) = 1 - \mu\kappa(a)$ for $a > 0$.
4. Set the feedback gains (g_i, h_i) for $i \in \mathbb{I}_m$ by

$$g_i := \frac{\mu k_i \mathfrak{g}_\ell(\omega)}{h_i}, \quad h_i := \frac{a|\mathfrak{h}_\ell(\omega)|}{\hat{y}_i}. \quad (15)$$

5. For the controller (μ, ω_o, g, h), the MHB equation has a solution $(\omega, \xi_\ell, \hat{\alpha})$ with $\hat{\alpha}_i := a|\mathfrak{h}_\ell(\omega)|/\mathfrak{h}_\ell(\omega)$.

Procedure 1 shows that the freedom in the control design, to achieve a prescribed mode shape $\hat{x} = \xi_\ell$, is embedded in the

triple (ω_o, η, μ). We aim to determine a condition on these parameters under which the resulting oscillation frequency ω is close to ω_ℓ so that natural entrainment to the specified mode is approximately achieved. Note that the parameters (ω_o, η) determine the value of ω in Step 2 of Procedure 1, while the parameter μ does not influence the oscillation frequency but simply scales the amplitude a of the q-oscillation as in Step 3. Thus, (ω_o, η) are identified as the essential controller parameters.

This conclusion is further justified by the fact that the stability property of the resulting oscillation can be estimated from (ω_o, η) only. In particular, the quasi-linear system associated with the CPG controller specified by (ω_o, η, μ) through Procedure 1 is given by (9) with

$$r_i(s) = \frac{4\eta(1 - \mathfrak{f}_\ell(\omega))k_i\omega_o s}{s^2 + 2\mathfrak{f}_\ell(\omega)\omega_o s + \omega_o^2}, \tag{16}$$

where ω is determined by $\mathfrak{g}_\ell(\omega) = \eta$ in Step 2 of Procedure 1. We see that the quasi-linear system, and therefore its marginal stability property as well, are independent of the choice of μ and are solely determined by (ω_o, η).

For this reason, we fix $\mu \geq 1$ arbitrarily in the rest of our discussion, and consider the effect of the essential controller parameters (ω_o, η) on the resulting oscillation frequency. The important question is what values of (ω_o, η) lead to natural entrainment approximately, i.e., $\omega \cong \omega_\ell$.

C. Mode Partition Diagram

In the design of the CPG controller, the pair (ω_o, η) must be chosen feasible, i.e., the equations in Steps 2 and 3 in Procedure 1 must be solvable for $\omega > 0$ and $a > 0$. Since the range of the function $\mathfrak{g}_\ell(\omega)$ on $\omega > 0$ is the entire set of real numbers [12], the equation in Step 2 is always solvable for $\omega > 0$. The solution may not be unique, and we will visit this issue shortly. Since $\psi \in \Psi$, the range of the describing function is $0 < \kappa(a) < 1$ on $a > 0$. Hence, a pair (ω_o, η) is feasible if and only if a solution ω to $\mathfrak{g}_\ell(\omega) = \eta$ (which always exists) satisfies

$$1 - \mu < \mathfrak{f}_\ell(\omega) < 1. \tag{17}$$

It appears difficult to obtain an exact characterization of the feasible set in a simple manner. However, if we replace (17) by

$$0 < \mathfrak{f}_\ell(\omega) < 1, \tag{18}$$

then a subset of the feasible set is given by

$$\mathbb{F}_\ell := \{ (\omega_o, \eta) \in \mathbb{R}^2 \mid \eta(\eta - \lambda_\ell(\omega_o)) > 0 \}, \\ \lambda_\ell(\omega_o) := \zeta_\ell \varpi, \tag{19}$$

where ζ_ℓ and ϖ are defined in (11). More precisely, one can show [12] that there exists $\omega > 0$ such that $\mathfrak{g}_\ell(\omega) = \eta$ and (18) hold if and only if $(\omega_o, \eta) \in \mathbb{F}_\ell$, and that such ω is given as the unique positive solution to $\mathfrak{g}_\ell(\omega) = \eta$. Let $\mathbb{F}$ be the union of $\mathbb{F}_\ell$ for all $\ell \in \mathbb{I}_n$. Although the set $\mathbb{F}$ may not include all the feasible domain, it covers a large portion of the whole parameter plane (ω_o, η). This can be seen by visualizing $\mathbb{F}$ in terms of its complement in $\mathbb{R}^2$, which comprises the line

$\eta = 0$, and the regions $\{(\omega_o, \eta) \mid \lambda_1(\omega_o) \leq \eta < 0, \ \omega_o < \omega_1\}$ and $\{(\omega_o, \eta) \mid 0 < \eta \leq \lambda_n(\omega_o), \ \omega_o > \omega_n\}$.

In addition to the feasibility, we need to ensure during the control design that (9) is marginally stable, and find a subset of $\mathbb{F}$ in which the stability requirement is satisfied. A necessary and sufficient condition for the marginal stability of (9) can be given as follows.

Lemma 2: Let $\ell \in \mathbb{I}_n$ and $(\omega_o, \eta) \in \mathbb{F}_\ell$ be given. Define the associated quasi-linear system by (9) and (16), where ω is the unique positive solution to $\mathfrak{g}_\ell(\omega) = \eta$. Then the quasi-linear system is marginally stable with a pair of poles at $\pm\jmath\omega$ and the rest in the open left half plane if and only if

$$\tau_\ell(\omega_o, \eta) > \tau_i(\omega_o, \eta), \quad \forall \ i \in \mathbb{I}_n \backslash \{\ell\}, \tag{20}$$

where τ_i is a function of (ω_o, η) and is defined for $i \in \mathbb{I}_n$ as follows. If $(\omega_o, \eta) \in \mathbb{F}_i$, let ω be the unique solution to $\mathfrak{g}_i(\omega) = \eta$ and set $\tau_i := \mathfrak{f}_i(\omega)$. If $(\omega_o, \eta) \notin \mathbb{F}_i$, then let $\tau_i := 0$.

A given pair $(\omega_o, \eta) \in \mathbb{F}$ may belong to multiple sets $\mathbb{F}_i$ for several values of i. In this case, Procedure 1 with $\ell := i$ will generate multiple controllers and predict the corresponding oscillation profiles. Lemma 2 states that at most one of these oscillations satisfies the marginal stability condition and it is the one having the largest value of $\tau_i(\omega_o, \eta)$. It can readily be seen from the basic equation $\tau_i = 1 - \mu\kappa(a)$ that τ_i is positively correlated with the amplitude a of the q-oscillation. Thus, the oscillation with the largest amplitude is expected to be stable.

Let us define the stable domain $\mathbb{S}$ to be the subset of the feasible domain $\mathbb{F}$ in the controller parameter space (ω_o, η) such that each element in $\mathbb{S}$ leads to a stable solution of the MHB equation. In view of Lemma 2, $\mathbb{S}$ is the union of $\mathbb{S}_\ell$ for all $\ell \in \mathbb{I}_n$, where

$$\mathbb{S}_\ell := \{(\omega_o, \eta) \in \mathbb{F}_\ell \mid \tau_\ell(\omega_o, \eta) > \tau_i(\omega_o, \eta), \ \forall \ i \in \mathbb{I}_n \backslash \{\ell\}\}. \tag{21}$$

Clearly, every two sets $\mathbb{S}_\ell$ and $\mathbb{S}_l$ are disjoint for $\ell \neq l$ because $(\omega_o, \eta) \in \mathbb{S}_\ell$ implies $\tau_\ell > \tau_l$ and hence $(\omega_o, \eta) \notin \mathbb{S}_l$. Also note that almost all elements of $\mathbb{F}$ belong to $\mathbb{S}$, with the exceptions being those (ω_o, η) for which the maximum of τ_i over i is attained by two or more values of i. In fact, one can show [30] that the difference between $\mathbb{F}$ and $\mathbb{S}$ is just a finite collection of lines in $\mathbb{R}^2$. Finally, each set $\mathbb{S}_\ell$ can be partitioned into regions with positive and negative gains η by noting that $\lambda_\ell(\omega_o)$ is a monotonically increasing function satisfying $\lambda_\ell(\omega_\ell) = 0$. In particular, η is positive/negative if $\omega_o - \omega_\ell$ is positive/negative. Now we have a summary.

Corollary 1: The following statements hold.

- The feasible domain $\mathbb{F}$ almost coincides with the stable domain $\mathbb{S}$ in the sense that, for each ω_o, there are at most a finite number of η such that $(\omega_o, \eta) \in \mathbb{F}\backslash\mathbb{S}$.
- The stable domain $\mathbb{S}$ can be partitioned into disjoint sets $\mathbb{S}_\ell$ for $\ell \in \mathbb{I}_n$.
- Each $\mathbb{S}_\ell$ can be partitioned into $\mathbb{O}_{\ell\ell}$ and $\mathbb{O}_{o\ell}$ with a

boundary $\mathbb{B}_\ell$, where

$$\mathbb{O}_{\ell\ell} := \{(\omega_o, \eta) \in \mathbb{S}_\ell \mid (\omega_o - \omega_\ell)(\eta - \lambda_\ell(\omega_o)) > 0\},$$
$$\mathbb{O}_{o\ell} := \{(\omega_o, \eta) \in \mathbb{S}_\ell \mid (\omega_o - \omega_\ell)\eta < 0\},$$
$$\mathbb{B}_\ell := \{(\omega_o, \eta) \in \mathbb{S}_\ell \mid \eta \neq 0, \ \omega_o = \omega_\ell\}. \tag{22}$$

The two sets $\mathbb{O}_{\ell\ell}$ and $\mathbb{O}_{o\ell}$ turn out to describe two parameter regions for approximate entrainment to the natural frequency ω_ℓ and to the intrinsic CPG frequency ω_o, respectively, with the mode shape being ξ_ℓ for both cases. It has been shown [12] that $\mathfrak{f}_\ell(\omega) := \varpi_o \varpi_\ell / \zeta_\ell$ is a strictly convex function such that $\mathfrak{f}_\ell(\omega_o) = \mathfrak{f}_\ell(\omega_\ell) = 0$. Hence, condition (18) can be visualized as two intervals near ω_o and ω_ℓ, where the length of each interval is small if ζ_ℓ is small. This means that if a controller is designed from $(\omega_o, \eta) \in \mathbb{F}_\ell$ and the closed-loop system has an oscillatory trajectory, then the frequency ω would be necessarily close to either the CPG frequency ω_o or the natural frequency ω_ℓ, provided the damping is small. A formal statement of this fact, given below, is a main result of this paper.

Theorem 1: Let $\ell \in \mathbb{I}_n$, $\mu \geq 1$, and $(\omega_o, \eta) \in \mathbb{S}_\ell$ be given, where $\mathbb{S}_\ell$ is defined by (21). Let a controller (μ, ω_o, g, h) and oscillation parameters $(\omega, \hat{\alpha})$ be (uniquely) determined by Procedure 1. Then, $(\omega, \xi_\ell, \hat{\alpha})$ is a stable solution to the MHB equation (10). Moreover, if $\omega_o \neq \omega_\ell$, then ω is close to either ω_ℓ or ω_o in the following sense:

$$\left| \frac{\omega - \omega_\ell}{\omega_\ell} \right| \leq \left| \frac{\zeta_\ell}{\varpi} \right| \quad \text{when} \quad (\omega_o, \eta) \in \mathbb{O}_{\ell\ell} \tag{23}$$

$$\left| \frac{\omega - \omega_o}{\omega_o} \right| \leq \left| \frac{\zeta_\ell}{\varpi} \right| \quad \text{when} \quad (\omega_o, \eta) \in \mathbb{O}_{o\ell}. \tag{24}$$

The feasible domain $\mathbb{F}$ in the controller parameter space (ω_o, η) can be partitioned into n regions $\mathbb{S}_\ell$ for $\ell \in \mathbb{I}_n$, in which the MHB analysis predicts that the resulting closed-loop system achieves entrainment to an oscillation (ω, ξ_ℓ) with stability. Each $\mathbb{S}_\ell$ can further be partitioned into two regions in which the oscillation frequency is close to either the natural frequency ω_ℓ or the CPG frequency ω_o. In particular, we have the oscillation (ω_ℓ, ξ_ℓ) in $\mathbb{O}_{\ell\ell}$, and (ω_o, ξ_ℓ) in $\mathbb{O}_{o\ell}$, approximately. The explicit characterizations of $\mathbb{O}_{\ell\ell}$ and $\mathbb{O}_{o\ell}$ allow us to calculate the boundaries and visually identify these regions for all $\ell \in \mathbb{I}_n$ on the (ω_o, η)-plane. We call this picture the *mode partition diagram*.

Figure 3 shows an example of such diagram for a three-link mechanical arm system (see Section V for details). The vertical lines indicate the natural frequencies. Each solid-colored area represents a region $\mathbb{O}_{\ell\ell}$, and each shaded area represents $\mathbb{O}_{o\ell}$. For instance, entrainment to the second mode of natural oscillation would be achieved approximately if the controller parameters are chosen at $(\omega_o, \eta) = (1, -1)$. On the other hand, if $(\omega_o, \eta) = (0.1, 1)$ are chosen, the resulting oscillation would have the first mode shape ξ_1, but the frequency would be close to the intrinsic CPG frequency $\omega_o = 0.1$ instead of the first mode $\omega_1 = 0.29$.

IV. Extension to General Mechanical Systems

We now remove Assumption 1 and consider a general class of mechanical systems. The collocation structure in
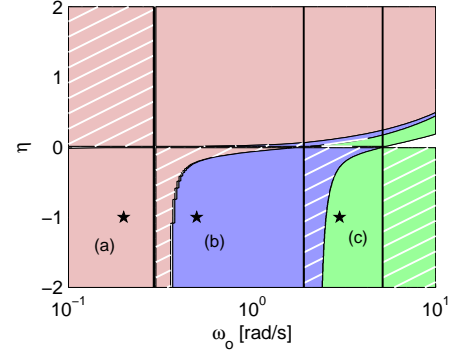

Fig. 3. An example of the mode partition diagram for a 3-DOF system ($\omega_1 = 0.292$, $\omega_2 = 1.92$, $\omega_3 = 5.15$); solid pink: $\mathbb{O}_{11}$, shaded pink: $\mathbb{O}_{o1}$, solid blue: $\mathbb{O}_{22}$, shaded blue: $\mathbb{O}_{o2}$, solid green: $\mathbb{O}_{33}$, shaded green: $\mathbb{O}_{o3}$

Assumption 1 made it easy to reduce the MHB equation into m sets of scalar equations for the m input/output channels as in Lemma 1. For the general case, it is not obvious if such decomposition is possible. It turns out, however, that it is indeed possible. The key idea is to define the stiffness $k_{\ell i}$ and damping $d_{\ell i}$ for each input/output channel i, with respect to a given mode shape ξ_ℓ:

$$k_\ell := Y_\ell^{-1} B^\dagger K \xi_\ell, \quad d_\ell := Y_\ell^{-1} B^\dagger D \xi_\ell,$$
$$\zeta_{\ell i} := \frac{\omega_\ell}{2} \left(\frac{d_{\ell i}}{k_{\ell i}} \right), \quad Y_\ell := \operatorname{diag}(C\xi_\ell), \tag{25}$$

where $i \in \mathbb{I}_m$, and $k_{\ell i}$ and $d_{\ell i}$ are the ith entries of vectors k_ℓ and d_ℓ, respectively. The rationale behind these definitions is as follows. When $x(t)$ sinusoidally oscillates with mode shape ξ_ℓ, the phasor of the stiffness force is given by $K\xi_\ell$. If this force were to be generated by springs collocated with the sensors and actuators, we should have $B\mathcal{K}C\xi_\ell = K\xi_\ell$, where $\mathcal{K}$ is a diagonal matrix with the stiffness of the ith input/output channel, $k_{\ell i}$, on the ith diagonal. A solution $\mathcal{K}$ to this equation, if any, is given by stacking $k_{\ell i}$ in (25) on the diagonal. For collocated systems satisfying Assumption 1, the parameters $k_{\ell i}$ and $d_{\ell i}$ are independent of ℓ and are given by k_i and ρk_i, consistently with our expectation. In the rest of this paper, we assume that $k_{\ell i}$ and $d_{\ell i}$ are positive for all $\ell \in \mathbb{I}_n$ and $i \in \mathbb{I}_m$.

With the definitions in (25), the MHB equation (10) can be split into m sets of scalar equations, analogously to Lemma 1 for the collocated case.

Lemma 3: Let the mechanical system (1), controller (2), and an oscillation profile $(\omega, \hat{x}, \hat{\alpha})$ be given. Suppose $\hat{x} = \xi_\ell$ for some $\ell \in \mathbb{I}_n$ and $\omega_\ell > 0$. Define the parameters in (25) and assume $k_{\ell i}, d_{\ell i} > 0$ and $h_i \hat{y}_i \neq 0$ for all $i \in \mathbb{I}_m$. When B has a full column rank, the MHB equation (10) is satisfied if and only if

$$(I - BB^\dagger)K\xi_\ell = 0 \quad \text{or} \quad \omega = \omega_\ell, \tag{26}$$
$$(I - BB^\dagger)D\xi_\ell = 0, \tag{27}$$
$$\mathfrak{f}_{\ell i}(\omega) = 1 - \mu\kappa(|\hat{\alpha}_i|), \ \mathfrak{g}_{\ell i}(\omega) = \frac{g_i h_i}{\mu k_{\ell i}}, \ \mathfrak{h}_{\ell i}(\omega) = \frac{h_i \hat{y}_i}{\hat{\alpha}_i}, \tag{28}$$

hold for all $i \in \mathbb{I}_m$, where

$$\mathfrak{f}_{\ell i}(\omega) := \frac{\varpi_o \varpi_\ell}{\zeta_{\ell i}}, \quad \mathfrak{g}_{\ell i}(\omega) := \frac{\omega \varpi_o(\varpi_\ell^2 + \zeta_{\ell i}^2)}{\omega_\ell(\varpi_o \varpi_\ell - \zeta_{\ell i})},$$

$$\mathfrak{h}_{\ell i}(\omega) := \varpi_o \left(\frac{\varpi_\ell}{\zeta_{\ell i}} + j \right). \tag{29}$$

When B does not have a full column rank, conditions (26) and (27) remain necessary, but (26)–(28) become only sufficient.

Condition $(I - BB^\dagger)K\xi_\ell = 0$ in (26) means that the stiffness force Kx during oscillations with the ℓth mode shape $x(t) = \Im[\xi_\ell e^{j\omega t}]$ is in the range space of B so that the set of actuators is able to provide the compensation necessary for modifying the force in any desired manner. A similar comment applies to condition (27) in terms of the damping force $D\dot{x}$. When underactuated, these conditions can be violated, in which case there is no controller of the uncoupled CPG structure that achieves oscillations with the mode shape ξ_ℓ. If the system is fully actuated (i.e., B has a full row rank), then the conditions are automatically satisfied because $BB^\dagger = I$, and this is why they do not show up in Lemma 1. Condition (28) is identical to those given in (12) for the collocated system, except that ζ_ℓ is now replaced by $\zeta_{\ell i}$. The damping ratio $\zeta_{\ell i}$ with respect to the mode shape ξ_ℓ may no longer be uniform over all input/output channels $i \in \mathbb{I}_m$. This complicates our theoretical developments to some extent, but a result essentially analogous to Theorem 1 can be obtained. To this end, let us consider essential controller parameters and their feasible and stable domains for general mechanical systems.

Following the development for the collocated systems, we may define $\eta_{\ell i} := g_i h_i/(\mu k_{\ell i})$ for $i \in \mathbb{I}_m$ to be the essential parameters. However, $\eta_{\ell i}$ depends on i in the general case, and hence does not serve for our purpose of capturing the essential design freedom by a minimal number of parameters. However, it turns out that one of these parameters $\eta_{\ell p}$ for an appropriately chosen $i := p$ can serve as the essential parameter η.

Procedure 2:

1. Let a desired mode of oscillation ℓ and the controller parameters ω_o, η, and μ be given.
2. Pick an integer $p \in \mathbb{I}_m$ and solve $\mathfrak{g}_{\ell p}(\omega) = \eta$ for $\omega > 0$.
3. For each $i \in \mathbb{I}_m$, solve $\mathfrak{f}_{\ell i}(\omega) = 1 - \mu\kappa(a_i)$ for $a_i > 0$.
4. Set the feedback gains (g_i, h_i) for $i \in \mathbb{I}_m$ by

$$g_i := \frac{\mu k_{\ell i} \mathfrak{g}_{\ell i}(\omega)}{h_i}, \quad h_i := \frac{a_i |\mathfrak{h}_{\ell i}(\omega)|}{\hat{y}_i}. \tag{30}$$

5. For the controller (μ, ω_o, g, h), the MHB equation has a solution $(\omega, \xi_\ell, \hat{\alpha})$ with $\hat{\alpha}_i := a_i |\mathfrak{h}_{\ell i}(\omega)|/\mathfrak{h}_{\ell i}(\omega)$.

Procedure 2 is basically the same as Procedure 1, with a major difference being that we now need to choose $p \in \mathbb{I}_m$. The index p should be chosen in such a way that ω obtained in Step 2 for a given $\eta \in \mathbb{F}_\ell$ guarantees existence of a_i in Step 3, where $\mathbb{F}_\ell$ is a feasible domain yet to be defined for the general case. Recall from the collocated case that $\mathfrak{f}_{\ell i}(\omega) = 1 - \mu\kappa(a_i)$ is solvable for $a_i > 0$ if and only if

$$1 - \mu < \frac{\varpi_o \varpi_\ell}{\zeta_{\ell i}} < 1.$$

Since $\mu \geq 1$ and $\zeta_{\ell i} > 0$, this condition holds for all $i \in \mathbb{I}_m$ if and only if it holds for $i = p$, where p is the integer that gives the smallest damping ratio, i.e.,

$$\zeta_\ell := \min_{i \in \mathbb{I}_m} \zeta_{\ell i} = \zeta_{\ell p}.$$

In this way, the index p in Step 2 can be uniquely chosen for a given ℓ. We can then define a feasible domain $\mathbb{F}_\ell$ as in (19), based on the fact that $\mathfrak{g}_{\ell i}(\omega) = \eta$ has a unique solution $\omega > 0$ and it satisfies $0 < \mathfrak{f}_{\ell i}(\omega) < 1$ if and only if $\eta(\eta - \zeta_{\ell i}\varpi) > 0$ holds.

Given $\ell \in \mathbb{I}_n$, $(\omega_o, \eta) \in \mathbb{F}_\ell$, and $\mu \geq 1$, Procedure 2 uniquely determines the feedback gains g and h as well as the resulting oscillation profile $(\omega, \xi_\ell, \hat{\alpha})$. As before, the parameter μ scales the oscillation amplitude of q_i but has no effect on the frequency. Moreover, it can be verified that the associated quasi-linear system defined by (8) and (9) is independent of the value of μ. Thus, we consider (ω_o, η) to be the essential controller parameters. As in the collocated case, the stable domain $\mathbb{S}_\ell$ is defined to be the subset of $\mathbb{F}_\ell$, in which the associated quasi-linear system satisfies the marginal stability condition. The main result for the general case is now stated.

Theorem 2: Let $\ell \in \mathbb{I}_n$, $\mu \geq 1$, and $(\omega_o, \eta) \in \mathbb{S}_\ell$ be given, where $\mathbb{S}_\ell$ is defined above. Suppose conditions (26) and (27) hold, and let a controller (μ, ω_o, g, h) and oscillation parameters $(\omega, \hat{\alpha})$ be (uniquely) determined by Procedure 2. Then, $(\omega, \xi_\ell, \hat{\alpha})$ is a stable solution to the MHB equation (10). Moreover, if $\omega_o \neq \omega_\ell$, then ω is close to either ω_ℓ or ω_o in the sense stated in (23) or (24), where $\mathbb{O}_{\ell\ell}$ and $\mathbb{O}_{o\ell}$ are defined in (22).

Theorem 2 is a generalization of Theorem 1 where the assumption of the collocated structure is removed. As before, the result allows us to draw mode partition diagrams, but there are certain limitations for the general case. The limitations arise mainly from the absence of a simple analytical characterization of the marginal stability condition like the one in Lemma 2, leading to the lack of the first two statements in Corollary 1.

For the collocated case, the feasible domain $\mathbb{F}$ of the controller parameter space practically coincides with the stable domain $\mathbb{S}$, and can be partitioned into disjoint sets $\mathbb{S}_\ell$ for $\ell \in \mathbb{I}_n$, in which entrainment to an oscillation with the ℓth mode shape is achieved. For the general case, it is difficult to derive a simple characterization of $\mathbb{S}_\ell$. Because of this, we were not able to determine whether $\mathbb{S}_\ell$ and $\mathbb{S}_l$ are disjoint for any $\ell \neq l$. There may be some overlap between the two regions, in which case, the same parameter (ω_o, η) can lead to two controllers achieving two different modes of oscillation. Also, there may be some nontrivial gap between $\mathbb{F}$ and $\mathbb{S}$. If the parameter (ω_o, η) happens to be chosen in the gap, then Procedure 2 will generate controller(s) for those ℓ such that $(\omega_o, \eta) \in \mathbb{F}_\ell$, but none of them will make the associated quasi-linear system marginally stable, and hence none of the resulting oscillations is expected to be stable.

In spite of these limitations, mode partition diagrams can still be generated. It can readily be checked whether or not a given pair $(\omega_o, \eta_\ell) \in \mathbb{F}_\ell$ belongs to $\mathbb{S}_\ell$ by numerically calculating the roots of the characteristic equation $\det(A(s)) = 0$. The partition of $\mathbb{S}_\ell$ into $\mathbb{O}_{\ell\ell}$ and $\mathbb{O}_{o\ell}$ is easily done using the

definitions in (22). The only difference from the collocated case at this numerical level is that two regions $\mathbb{S}_\ell$ and $\mathbb{S}_l$ could overlap to each other, and this may require a separate figure for each $\mathbb{S}_\ell$ to clearly indicate the region.

V. NUMERICAL EXAMPLE

Consider a mechanical arm on a horizontal plane, formed as a chain of three rigid links connected by two rotational joints to each other. The ith link has mass m_i and length $2\ell_i$, and the first link is connected to the inertial frame through a rotational joint. Mounted at the ith joint are a spring of stiffness k_i, a dashpot of damping coefficient ρk_i, and an actuator that generate torque input u_i. The equation of motion is then given by

$$J_x \ddot{x} + G_x \dot{x}^2 + D\dot{x} + Kx = Bu, \quad y = Cx, \quad (31)$$

where x_i is the angular displacement of the ith link, y_i is the relative angle between the ith and $(i+1)^{\text{th}}$ links, $\dot{x}^2$ is the vector whose i^{th} entry is $\dot{x}_i^2$, and

$$J_x := J_o + S_x Q S_x + C_x Q C_x, \quad G_x := S_x Q C_x - C_x Q S_x,$$
$$Q := L^\mathsf{T} M L, \quad C := B^\mathsf{T}, \quad K := B\mathcal{K}C, \quad D := \rho K,$$
$$M := \text{diag}(m_1, m_2, m_3), \quad \mathcal{K} := \text{diag}(k_1, k_2, k_3),$$
$$J_o := \text{diag}\left(m_1\ell_1^2, m_2\ell_2^2, m_3\ell_3^2\right)/3,$$
$$S_x := \text{diag}(\sin x_1, \sin x_2, \sin x_3),$$
$$C_x := \text{diag}(\cos x_1, \cos x_2, \cos x_3),$$
$$B := \begin{bmatrix} 1 & -1 & 0 \\ 0 & 1 & -1 \\ 0 & 0 & 1 \end{bmatrix}, \quad L := \begin{bmatrix} \ell_1 & 0 & 0 \\ 2\ell_1 & \ell_2 & 0 \\ 2\ell_1 & 2\ell_2 & \ell_3 \end{bmatrix}.$$

We use the following parameter values:

$$\ell_i = 0.5, \quad m_i = 1.0, \quad k_i = 1.0, \quad \rho = 0.1,$$

for $i \in \mathbb{I}_3$. By linearizing (31) around the origin, we obtain (1) with $J := J_o + Q$, and its natural modes (ω_ℓ, ξ_ℓ) are given by Table I. The mode partition diagram for the link system are given by Fig. 3. Based on this diagram, we selected the controller parameters (ω_o, η) as (a), (b) and (c) in Table II so that the entrained oscillation profiles are close to the 1$^{\text{st}}$, 2$^{\text{nd}}$ and 3$^{\text{rd}}$ natural modes, respectively. For each case, we have designed the feedback gains (g, h) by (15), where $\mu = 1.5$ and $\psi(x) = \tanh(x)$.

TABLE I
NATURAL MODES OF THE MECHANICAL ARM

ℓ	1$^{\text{st}}$ mode	2$^{\text{nd}}$ mode	3$^{\text{rd}}$ mode
ω_ℓ	0.292	1.92	5.15
ξ_ℓ	$\begin{bmatrix} 0.402 \\ 0.615 \\ 0.678 \end{bmatrix}$	$\begin{bmatrix} 0.476 \\ -0.242 \\ -0.846 \end{bmatrix}$	$\begin{bmatrix} 0.291 \\ -0.654 \\ 0.698 \end{bmatrix}$

First, the accuracy of the MHB method has been evaluated in comparison with simulations of the linearized system (1). In each case, a steady state oscillation of $x(t)$ was observed, and was approximated by Fourier series truncation $x(t) \cong \Im[\hat{x}_{\text{SIM}} e^{j\omega_{\text{SIM}}(t-t_o)}]$, where the time shift t_o was chosen so that the imaginary part of the phasor vector $\hat{x}_{\text{SIM}}$ has a minimum

TABLE II
FEEDBACK GAINS DESIGNED FOR THE THREE MODES

	(a)	(b)	(c)
ℓ	1	2	3
(ω_o, η)	$(0.2, -1.0)$	$(0.5, -1.0)$	$(3.0, -1.0)$
g	$\begin{bmatrix} 0.0118 \\ 0.00627 \\ 0.00184 \end{bmatrix}$	$\begin{bmatrix} 0.0406 \\ 0.0612 \\ 0.0515 \end{bmatrix}$	$\begin{bmatrix} 0.0913 \\ 0.296 \\ 0.424 \end{bmatrix}$
h	$\begin{bmatrix} -127 \\ -239 \\ -813 \end{bmatrix}$	$\begin{bmatrix} -36.9 \\ -24.5 \\ -29.1 \end{bmatrix}$	$\begin{bmatrix} -16.4 \\ -5.06 \\ -3.54 \end{bmatrix}$

norm. The results are summarized in Table III, where ω_{MHB} is the estimated frequency, and the errors are defined by

$$e_{\text{PRD}} := \frac{|\omega_{\text{MHB}} - \omega_{\text{SIM}}|}{\omega_{\text{SIM}}}, \quad e_\omega := \frac{|\omega_{\text{SIM}} - \omega_\ell|}{\omega_\ell},$$
$$e_x := \frac{\|\bar{x}_{\text{SIM}} - \xi_\ell\|}{\|\xi_\ell\|}, \quad \bar{x}_{\text{SIM}} := \frac{\hat{x}_{\text{SIM}}}{\|\hat{x}_{\text{SIM}}\|}.$$

We see that the errors e_{PRD} and e_x are small, and the error bound $e_\omega < \zeta_\ell/\varpi$ is satisfied. Thus, the MHB method provided fairly accurate result. Next, we simulated the original

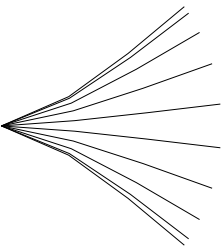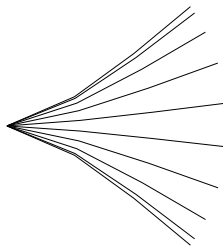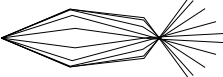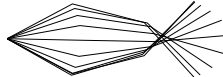TABLE III
EVALUATION BY LINEAR SIMULATIONS
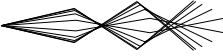
	ω_{MHB}	ω_{SIM}	e_{PRD}	e_ω	e_x	ζ_ℓ/ϖ
(a)	0.30	0.30	0.1%	3.3%	0.0%	3.8
(b)	1.99	1.99	0.2%	3.9%	0.3%	5.4
(c)	6.25	6.17	1.2%	20.0%	4.3%	45.4

TABLE IV
NONLINEAR SIMULATION RESULTS

	$\|\hat{x}_{\text{SIM}}\|$	ω_{SIM}	ω_{NAT}
(a)	1.02	0.30	0.29
(b)	1.02	1.58	1.56
(c)	0.95	3.98	2.91

system (31) with (g, h) designed above to evaluate applicability of the MHB method for nonlinear systems, for which a natural oscillation is defined as a periodic initial state response with $\dot{x}(0) = 0$ and $\rho = 0$. The simulated oscillations are compared with the natural oscillations numerically found by searching for an initial displacement x_o and period T such that $f(x_o, T) := \|x(T) - x_o\|^2 + \|\dot{x}(T)\|^2 = 0$ when $x(0) = x_o$ and $\dot{x}(0) = 0$. To find a particular mode, $f(x_o, T)$ was minimized using "fminsearch" in Matlab with the initial point of optimization set from the corresponding mode shape of the linearized system. This involved optimization with four scalar parameters in $x_o \in \mathbb{R}^3$ and $T \in \mathbb{R}$ with the objective function value $f(x_o, T)$ evaluated by simulation of a nonlinear system with six state variables. More details are described in [30]. Snapshots of the simulated oscillations and the natural oscillations during a half period are depicted in Table V. The simulated frequency ω_{SIM}, oscillation amplitude $\|\hat{x}_{\text{SIM}}\|$, and natural frequency ω_{NAT} are summarized in Table IV. Although ω_{SIM} is not very close to ω_{NAT} for (c), the oscillation shapes in Table V are similar. Thus, we conclude that the CPG controller roughly achieved the natural entrainment for the nonlinear system (31).

TABLE V
NONLINEAR MODE SHAPES AND ACHIEVED OSCILLATIONS

	Natural Modes	Simulation Results
(a)		
(b)		
(c)		

VI. DISCUSSION

A. Control Mechanisms for Natural Entrainment

We have identified (ω_o, η) to be the essential controller parameters, and found regions $\mathbb{O}_{\ell\ell}$ with $\ell \in \mathbb{I}_n$ on the parameter plane in which entrainment to the ℓth mode of natural oscillation is achieved approximately. The definition of $\mathbb{O}_{\ell\ell}$ in (22) reveals that the feedback gain η should be positive/negative when ω_o is chosen to be greater/smaller than ω_ℓ:

$$\begin{cases} \omega_o > \omega_\ell & \Rightarrow \quad \eta > \zeta_\ell \varpi > 0, \\ \omega_o < \omega_\ell & \Rightarrow \quad \eta < \zeta_\ell \varpi < 0. \end{cases} \quad (32)$$

Moreover, a bound is obtained on the entrainment error, which is defined as the difference between the targeted natural frequency ω_ℓ and the actual oscillation frequency ω. The error bound $|\zeta_\ell/\varpi|$ in (23) is smaller if the damping ratio ζ_ℓ is smaller and $|\varpi|$ is larger. The parameter $|\varpi|$ can be thought of as the distance between ω_o and ω_ℓ. Thus, closer entrainment to a natural mode is expected if ω_o is chosen away from the desired natural frequency ω_ℓ. Below, we shall give physical interpretations to these findings by probing into the control mechanisms underlying natural entrainment. Some preliminary discussions for one-DOF systems can be found in [12].

Let us first examine the role of the CPG unit when it is achieving natural entrainment to the ℓth mode approximately. Recall that the transfer function of the CPG unit, quasi-linearized through the describing function, is given by $r_i(s)$ in (8). It is straightforward to show, using (28), that $r_i(\jmath\omega) \cong \jmath\omega d_{\ell i}$ holds when the oscillation frequency ω is close to ω_ℓ. Hence, during the natural entrainment, the control input $u_i = r_i(s)y_i \cong d_{\ell i}\dot{y}_i$ acts as a positive rate feedback to provide negative damping that cancels the mechanical damping. It should be noted that the cancellation is specifically tuned for $d_{\ell i}$, the damping of the ith input/output channel during oscillation with the mode shape ξ_ℓ. With the damping for the ℓth mode removed, the closed-loop system would have an oscillatory solution near the natural mode. This situation corresponds to the fact that the quasi-linear system (9) has a pair of poles at $s = \pm\jmath\omega$ with $\omega \cong \omega_\ell$.

The marginal stability condition ensures that the poles at $s = \pm\jmath\omega$ are the only ones on the imaginary axis and the rest are in the open left half plane. Hence, with almost all initial conditions, the trajectory of the quasi-linear system converges to an oscillation $x(t) = \Im[\xi_\ell c e^{\jmath\omega t}]$ where c is an amplitude scaling factor that depends on the initial condition. Structural stability of the oscillation resulting for the original nonlinear system (convergence to a fixed orbit regardless of the initial condition) is also expected from the MHB analysis, and has been confirmed by numerical simulations for some example systems (one reported in the previous section; see [30] for others). The mechanism of stabilization can be seen in the quasi-linear $r_i(s)$ which depends on the amplitude a_i of the q_i-oscillation. For a fixed a_i, the transfer function $r_i(s)$ is a band-pass filter with the center frequency ω_o and the peak gain $|r_i(\jmath\omega_o)| = 2g_i h_i \kappa_i/(1 - \mu\kappa_i)$. When the amplitude a_i is positively perturbed, κ_i decreases and the gain of $r_i(s)$ reduces. This results in reduced effects of negative damping, leading to reduction in a_i. By an analogous argument, a negative perturbation of a_i results in tendency to increase a_i. Thus, stability of oscillation can be explained through amplitude-dependent negative damping supplied by the nonlinear feedback control.

A quasi-linear analysis of $r_i(s)$ further reveals control principles behind (32) and the requirement of a large separation between ω_o and ω_ℓ for closer entrainment. When $\eta > 0$, the phase plot of $r_i(\jmath\omega)$ monotonically decreases from $+90^o$ to -90° as ω increases, passing through 0° at $\omega = \omega_o$. Hence, if $\omega_o \gg \omega_\ell$, then $r_i(s)$ has a phase close to $+90^o$ near ω_ℓ, acting like an approximate differentiator as discussed above. We see that this approximation is more accurate if ω_o is much larger than ω_ℓ, explaining why $\omega_o \gg \omega_\ell$ is desired for closer entrainment. On the other hand, when $\eta < 0$, the phase plot of $r_i(\jmath\omega)$ monotonically increases from -90° to $+90^o$. Therefore, choosing $\omega_o \ll \omega_\ell$ would make the phase close to $+90^o$ near ω_ℓ as desired. In this case, however, the gain plot of $r_i(s)$ near ω_ℓ has a negative slope, and hence $r_i(s)$ acts like an integrator with a negative gain, rather than a differentiator with a positive gain.

Thus, the simplest control mechanisms that could capture the essence of the CPG dynamics would be the positive rate feedback $u_i = \psi(\dot{y}_i)$ and negative integral feedback $u_i = -\psi(\int y_i dt)$, where amplitude-dependent gains are realized by a sigmoid function ψ. While these control laws may well explain the entrainment mechanisms for one-DOF systems [12], they do not seem sufficient for multi-DOF systems due to the lack of ability to distinguish different modes. The quasi-linear analysis of the CPG unit suggests that the simplest control law for multi-DOF systems would be $u_i = \eta\psi(\beta(s)y_i)$, where $\beta(s)$ is a transfer function for a band-pass filter with center frequency ω_o, and η is a positive or negative feedback gain. For the CPG control, the mode partition diagram has shown that ω_o must be chosen appropriately to achieve entrainment to a specific mode; a rough rule of thumb from Fig. 3 would be to choose ω_o in the interval $\omega_{\ell-1} < \omega_o < \omega_\ell$, with negative feedback ($\eta < 0$), when (ω_ℓ, ξ_ℓ) is the targeted oscillation.

B. Limitations and Extensions

In the literature, methods for pattern analysis and synthesis of CPGs (or general nonlinear oscillators) have been developed. Classical techniques include the perturbation theory and averaging [31], [32], Poincaré-Bendixson theorem [14], Hopf bifurcation theorem [33], and the Malkin theorem for phase coupled oscillators [34]–[36]. More recent methods include integral quadratic constraints [37] and contraction analysis [38], [39]. These results are effective for analysis of dynamical systems, but do not seem directly useful for synthesis of (artificial) CPGs to control mechanical systems.

Given the extreme difficulty in rigorous analysis or design of limit cycles at a practically useful level, it appears reasonable to take an approximate approach as a viable direction. Our results are based on the MHB method that approximates periodic signals by sinusoids and static nonlinearities by describing functions. Therefore, there is no theoretical guarantee for convergence to the prescribed mode of natural oscillation, or even for existence of a limit cycle near the natural mode or elsewhere. Nevertheless, the MHB method has allowed us to gain insights into fundamental control mechanisms underlying natural entrainment as discussed in the previous section. Moreover, the approximate conditions have been shown useful through a number of numerical examples [30], [40] for practical design of feedback control systems to achieve oscillations.

While our design conditions do not guarantee existence of a periodic orbit, we can formally prove existence of an oscillation in the sense of Yakubovich, which is known as the *Y-oscillation* [25]. An autonomous system with state variables $x(t) \in \mathbb{R}^n$ is said to be *Y-oscillatory* [41] if every trajectory is bounded and at least one of the variables $x_i(t)$ satisfies

$$\varliminf_{t \to \infty} x_i(t) < \varlimsup_{t \to \infty} x_i(t)$$

for almost all initial state $x(0)$. In general, this condition does not imply existence of a limit cycle, and a Y-oscillation could be a chaotic behavior. Nevertheless, this definition of oscillation appears to serve well for practical purposes [21], [42], [43]. It turns out that the closed-loop system (4) with a CPG controller in Theorem 1 is Y-oscillatory.

Theorem 3: Let the mechanical system (1), $\ell \in \mathbb{I}_n$, and $(\omega_o, \eta) \in \mathbb{F}_\ell$ be given, where Assumption 1 holds. Define the CPG controller (2) through Procedure 1. Suppose the origin of the closed-loop system (4) is a hyperbolic equilibrium. Then, the system is Y-oscillatory.

A proof of this result is given in the appendix, but the basic idea is the following. Using the fact that ψ is bounded, and $b(s)$ and (1) are stable, it can be shown that every trajectory is bounded. Due to $\psi(0) = 0$ and $b(0) = 0$, the origin is the unique equilibrium of (4). Hence, if the origin is hyperbolic and unstable, then for almost all initial conditions, the trajectory cannot converge to a fixed point, nor diverge to infinity, resulting in Y-oscillation.

A further generalization may be possible using a classical result (Theorem 5.2.15 in [44]) that guarantees existence of a periodic solution by a harmonic balance equation with additional conditions. This result also provides a bound on

the error between the predicted sinusoidal oscillation and the periodic trajectory. However, such developments appear to be nontrivial and may suffer from technical difficulties in obtaining the additional conditions in a less conservative, analytically insightful or numerically tractable manner.

Another direction for extending our results is toward a general theory of feedback control by CPGs. This paper has focused on control by a set of simple CPG units (reciprocal inhibition oscillators) that are not directly coupled to each other. We have shown that the CPG has a potential to provide a viable nonlinear control architecture for achieving coordinated oscillations that conform to mechanical constraints (i.e., natural motions). It would be interesting to examine how communications among multiple CPG units can contribute to broadening the class of achievable oscillation profiles to include, for instance, traveling waves observed during animal locomotion [45]. Such oscillation profiles can be characterized in terms of complex phasors $\hat{x}$ within the MHB framework [21], as a generalization of the real mode shape ξ_ℓ considered here. Systematic design of the interconnection structure for CPGs to achieve arbitrary oscillation profiles for mechanical systems would be a challenging open problem left for further research.

VII. Conclusion

We have developed a method for the design of feedback control systems with a decentralized CPG structure (2) to achieve entrainment to a prescribed mode of natural oscillation for n-DOF linear mechanical systems (1). The method is based on an MHB equation and hence there is no theoretical guarantee for our results (except for Theorem 3). Nevertheless, our numerical experience [30] seems to indicate their practical usefulness. An illustrative example was presented herein. Moreover, analytical insights are obtained for the control mechanisms underlying natural entrainment, as discussed in the previous section.

For the control design, the intrinsic CPG frequency ω_o and the feedback gain η have been identified as the essential parameters. The main results (Theorems 1 and 2) have shown, within the MHB framework, that the parameter plane (ω_o, η) can be partitioned into $2n$ regions $\mathbb{O}_{\ell\ell}$ and $\mathbb{O}_{o\ell}$ with $\ell \in \mathbb{I}_n$ as in (22), in which entrainment to oscillations (ω_ℓ, ξ_ℓ) and (ω_o, ξ_ℓ), respectively, are approximately achieved. This leads to mode partition diagrams (e.g., Fig. 3) that facilitate the control design. A bound on the entrainment error in the oscillation frequency has also been obtained, suggesting that the error would be small if ω_o is chosen away from the targeted natural frequency ω_ℓ.

APPENDIX A
PRELIMINARY LEMMAS

Lemma 4 (Marginal stability of the quasi-linear system): Let the mechanical system (1), CPG controller (2), $\omega, a \in \mathbb{R}_+$, and $\ell \in \mathbb{I}_n$ be given, where $\psi \in \Psi$ and Assumption 1 holds. Consider the quasi-linear system in (9). Suppose there exist $a \in \mathbb{R}_+$ and $\eta \in \mathbb{R}$ such that $g_i h_i = \mu k_i \eta$ holds for all $i \in \mathbb{I}_n$,

$i \in \mathbb{I}_m$, and

$$\kappa(a) = (1 - \mathfrak{f}_\ell(\omega))/\mu, \quad \eta = \mathfrak{g}_\ell(\omega) \quad (33)$$

are satisfied. Then, (9) has characteristic roots at $s = \pm\jmath\omega$. Moreover, the remaining roots are all in the open left half plane if and only if

$$-\min(\epsilon_{n+1}, \epsilon_i) < \mathfrak{f}_\ell(\omega), \quad (34)$$
$$\mathfrak{g}_i(\mathfrak{w}_i^+) < \mathfrak{g}_\ell(\omega) < \mathfrak{g}_i(\mathfrak{w}_i^-), \quad (35)$$

hold for all $i \in \mathbb{I}_n \setminus \{\ell\}$, where $\mathfrak{w} = \mathfrak{w}_i^\pm$ are the unique positive solutions of $\mathfrak{f}_i(\mathfrak{w}) = \mathfrak{f}_\ell(\omega)$ with $\mathfrak{w}_i^- < \mathfrak{w}_i^+$, and ϵ_i for $i \in \mathbb{I}_{n+1}$ are defined by

$$\epsilon_i := \frac{1}{2\rho\omega_i}\left(\sqrt{\frac{\omega_o}{\omega_i}} - \sqrt{\frac{\omega_i}{\omega_o}}\right)^2, \quad \omega_{n+1} := \frac{\omega_o}{1 + \rho\omega_1}.$$

Proof: Exploiting the collocated structure of the system (1), $A(s)$ in (9) can be written as

$$A(s) = Js^2 + Ke(s), \quad e(s) := 1 + \rho s + \frac{2\eta}{\mu - 1/(b(s)\kappa_o)},$$

where $\kappa_o := \kappa(a)$. By definition of the natural frequencies, the characteristic equation is given by

$$\det A(s) = 0 \Leftrightarrow s^2 + \omega_i^2 e(s) = 0$$
$$\Leftrightarrow s^4 + c_3 s^3 + c_2 s^2 + c_1 s + c_0 = 0 \quad (36)$$

for all $i \in \mathbb{I}_n$, where

$$c_3 := 2\omega_o(1 - \mu\kappa_o) + \rho\omega_i^2,$$
$$c_2 := \omega_o^2 + \omega_i^2 + 2\rho\omega_o\omega_i^2(1 - \mu\kappa_o),$$
$$c_1 := 2\omega_o\omega_i^2(1 - \mu\kappa_o - 2\mu\eta\kappa_o) + \rho\omega_o^2\omega_i^2, \quad c_0 := \omega_o^2\omega_i^2.$$

Substituting the expressions for κ_o and η given by (33), these coefficients can be written as

$$c_3 = 2\omega_o(\mathfrak{f}_\ell(\omega) + \beta_i), \quad c_2 = 2\rho\omega_o\omega_i^2(\mathfrak{f}_\ell(\omega) + \vartheta_i),$$
$$c_1 = \frac{2\omega_o\omega_i^2\omega^2}{\omega_\ell^2}(\mathfrak{f}_\ell(\omega) + \beta_\ell), \quad (37)$$

where $\mathfrak{f}_\ell(\omega)$ is defined by (14), and for $i \in \mathbb{I}_n$,

$$\beta_i := \frac{2}{\rho\omega_o}\zeta_i^2, \quad \zeta_i := \frac{\rho\omega_i}{2}, \quad \vartheta_i := \frac{1}{2\rho\omega_i}\left(\frac{\omega_o}{\omega_i} + \frac{\omega_i}{\omega_o}\right). \quad (38)$$

Let us first consider the characteristic roots of (36) for the case $i = \ell$. It can readily be verified that (36) reduces to

$$(s^2 + \omega^2)\left(s^2 + 2\omega_o(\mathfrak{f}_\ell(\omega) + \beta_\ell)s + \frac{\omega_o^2\omega_\ell^2}{\omega^2}\right) = 0.$$

Thus, there exist characteristic roots at $s = \pm\jmath\omega$, and the other two are in the open left half plane if and only if $\mathfrak{f}_\ell(\omega) > -\beta_\ell$. Next, consider the case $i \neq \ell$. By the Routh's stability criterion, all the roots of (36) are in the open left half plane if and only if

$$c_i > 0, \quad c_3 c_2 > c_1, \quad c_3 c_2 c_1 > c_1^2 + c_3^2 c_0,$$

for all $i \in \mathbb{I}_4$. The second condition is redundant because it is implied by the first and third, which are satisfied if and only if

$$-\min(\beta_\ell, \beta_i, \vartheta_i) < \mathfrak{f}_\ell(\omega), \quad \lambda^2 - 2c\lambda + (\omega_o/\omega_i)^2 < 0, \quad (39)$$

where

$$c := \rho\omega_o(\mathfrak{f}_\ell(\omega) + \vartheta_i), \quad \lambda := \left(\frac{\omega}{\omega_\ell}\right)^2 \frac{\mathfrak{f}_\ell(\omega) + \beta_\ell}{\mathfrak{f}_\ell(\omega) + \beta_i}.$$

Let $\chi^\pm := c \pm \sqrt{c^2 - (\omega_o/\omega_i)^2}$, and we obtain

$$\lambda^2 - 2c\lambda + (\omega_o/\omega_i)^2 < 0$$
$$\Leftrightarrow \chi^- < \lambda < \chi^+, \quad c^2 - (\omega_o/\omega_i)^2 > 0$$
$$\Leftrightarrow \mathfrak{g}_i(\mathrm{w}_i^+) < \mathfrak{g}_\ell(\omega) < \mathfrak{g}_i(\mathrm{w}_i^-), \quad \mathfrak{f}_\ell(\omega) + \epsilon_i > 0,$$

noting that

$$\mathfrak{g}_i(\omega) = \frac{1}{2(\mathfrak{f}_i(\omega) - 1)}\left\{\left(\mathfrak{f}_i(\omega) + \zeta_i\frac{\omega_i}{\omega_o}\right)\left(\frac{\omega}{\omega_i}\right)^2 - \left(\mathfrak{f}_i(\omega) + \frac{\rho}{2}\omega_o\right)\right\},$$

$$\chi^\pm = \left(\frac{\mathrm{w}_i^\pm}{\omega_i}\right)^2, \quad \mathfrak{f}_\ell(\omega) = \mathfrak{f}_i(\mathrm{w}_i^\pm).$$

Since $\epsilon_i = \vartheta_i - (1/\rho\omega_i) < \vartheta_i$, condition (39) is equivalent to (35) and $-\min(\beta_\ell, \beta_i, \epsilon_i) < \mathfrak{f}_\ell(\omega)$. This is the stability condition for (36) when $i \neq \ell$. Finally, combining the above two cases $i = \ell$ and $i \neq \ell$, we conclude the result where we note that $\min(\beta_i) = \epsilon_{n+1}$. ∎

Lemma 5 (Instability of the origin): Let the mechanical system (1) and CPG controller (2) be given, where $\psi \in \Psi$ and Assumption 1 holds. Suppose there exists a nonzero $\eta \in \mathbb{R}$ such that $g_i h_i = \mu k_i \eta$ holds for all $i \in \mathbb{I}_m$. Then the origin of the closed-loop system (4) is unstable if there exists $i \in \mathbb{I}_n$ such that at least one of the following conditions is violated:

$$\gamma_i \leq \beta_i, \quad \gamma_i \leq \delta_i, \quad \mathfrak{g}_i(\mathfrak{w}_i^+) \leq \eta \leq \mathfrak{g}_i(\mathfrak{w}_i^-), \quad (40)$$

where $(\mathfrak{f}_i, \mathfrak{g}_i)$, ζ_i, and β_i are defined by (14) and (38),

$$\gamma_i := \mu - 1, \quad \delta_i := \frac{(\omega_o - \omega_i)^2}{4\omega_o\omega_i\zeta_i}, \quad (41)$$

and $\omega = \mathfrak{w}_i^\pm$ are the positive roots of $\mathfrak{f}_i(\omega) = -\gamma_i$ with $\mathfrak{w}_i^- \leq \mathfrak{w}_i^+$, whose existence is guaranteed by $\gamma_i \leq \delta_i$.

Proof: Since $\psi'(0) = 1$, the linearized system of (4) around the origin is given by $\mathcal{G}(s, I)z = 0$, or equivalently, by $A(s)x = 0$ in (9) with $\kappa_i = 1$ for all $i \in \mathbb{I}_m$. Following the proof of Lemma 4, the linearized system is stable if and only if the characteristic roots of (36) are in the open left half plane. Since the characteristic equation (36) has exactly the same form as the one considered for the single DOF case in Lemma A.3 of [12], the result can be proved by slightly modifying the proof of this previous result. ∎

APPENDIX B
PROOFS OF LEMMAS AND THEOREMS

Proof of Lemma 1: With $\hat{x} = \xi_\ell$, condition $A(\jmath\omega)\hat{x} = 0$ in (10) can be written as

$$BR(\jmath\omega)C\xi_\ell = (K - \omega^2 J + \jmath\omega D)\xi_\ell,$$
$$\Leftrightarrow BR(\jmath\omega)\hat{y} = \sigma_\ell(\omega)K\xi_\ell = \sigma_\ell(\omega)B\mathcal{K}\hat{y},$$
$$\Leftrightarrow r_i(\jmath\omega) = k_i\sigma_\ell(\omega), \quad \text{for all } i \in \mathbb{I}_n, \quad (42)$$

where we used Assumption 1 and noted the definitions $\hat{y} = C\xi_\ell$ and $J\xi_\ell = K\xi_\ell/\omega_\ell^2$, and

$$\sigma_\ell(\omega) := 2(\omega/\omega_\ell)(\jmath\zeta_\ell - \varpi_\ell).$$

From (8), we have $r_i(\jmath\omega) = 2g_i\kappa_i p_i(\jmath\omega/\omega_o)$ with

$$p_i(\jmath\omega/\omega_o) = \frac{h_i}{1 - \mu\kappa_i + \jmath\varpi_o}. \tag{43}$$

Direct substitution of this expression into (42) yields

$$g_i h_i \kappa_i = (\omega/\omega_\ell)(\jmath\zeta_\ell - \varpi_\ell)(1 - \mu\kappa_i + \jmath\varpi_o)k_i.$$

The imaginary and real parts of this equation give the first and second equations in (12). Finally, substituting (43) into $\hat{\alpha}_i = p_i(\jmath\omega/\omega_o)\hat{y}_i$ in (10), and using the relation $1 - \mu\kappa_i = \varpi_o\varpi_\ell/\zeta_\ell$, we have the third equation in (12). ∎

Proof of Lemma 2: Since $(\omega_o, \eta) \in \mathbb{F}_\ell$, the solution $\omega > 0$ to $\eta = \mathfrak{g}_\ell(\omega)$ exists, is unique, and satisfies $0 < \mathfrak{f}_\ell(\omega) < 1$ [12]. Thus, (34) in Lemma 4 is satisfied. It then suffices to show the equivalence:

$$\mathfrak{g}_i(\mathfrak{w}_i^+) < \mathfrak{g}_\ell(\omega) < \mathfrak{g}_i(\mathfrak{w}_i^-) \; \Leftrightarrow \; \tau_\ell(\omega_o, \eta) > \tau_i(\omega_o, \eta), \tag{44}$$

for $i \in \mathbb{I}_n \setminus \{\ell\}$, where $\mathfrak{w} = \mathfrak{w}_i^\pm$ are defined in Lemma 4, and τ_i for $i \in \mathbb{I}_n$ are defined in Lemma 2.

Fix $i \in \mathbb{I}_n \setminus \{\ell\}$ and let $\mathfrak{w} = \mathfrak{w}_\zeta^\pm$ be the positive solutions of $\mathfrak{f}_i(\mathfrak{w}) = 1$ with $\mathfrak{w}_\zeta^- < \mathfrak{w}_\zeta^+$. Define $\mathfrak{w}_m := \min(\omega_o, \omega_i)$ and $\mathfrak{w}_M := \max(\omega_o, \omega_i)$, and introduce the two open intervals on the real axis

$$L := (\mathfrak{w}_\zeta^-, \mathfrak{w}_m), \quad R := (\mathfrak{w}_M, \mathfrak{w}_\zeta^+).$$

Note that $\mathfrak{f}_i(\mathfrak{w}_i^\pm) > 0$ is guaranteed by $\mathfrak{f}_\ell(\omega) > 0$, and $\mathfrak{w}_i^- \in L$ and $\mathfrak{w}_i^+ \in R$ [12] hold true since $\mathfrak{f}_i(\omega)$ is strictly convex and vanishes at $\omega = \omega_o$ and $\omega = \omega_\ell$ [12].

First, consider the case $\mathfrak{g}_\ell(\omega) < 0$. Let $\mathrm{w} = \mathrm{w}_i^+$ be the solution of $\mathfrak{g}_i(\mathrm{w}) = \eta$. Due to the strictly decreasing property of $\mathfrak{g}_i$ in R and the strictly increasing property of $\mathfrak{f}_i$ in R [12], we obtain

$$\begin{aligned}
& \mathfrak{g}_i(\mathfrak{w}_i^+) < \mathfrak{g}_\ell(\omega) = \eta \;\; \Leftrightarrow \;\; \mathfrak{w}_i^+ > \mathrm{w}_i^+ \\
\Leftrightarrow \;\; & \mathfrak{f}_i(\mathfrak{w}_i^+) > \mathfrak{f}_i(\mathrm{w}_i^+) \;\;\;\;\;\; \Leftrightarrow \;\; \tau_\ell(\omega_o, \eta) > \tau_i(\omega_o, \eta).
\end{aligned}$$

Next, consider the case $\mathfrak{g}_\ell(\omega) > 0$. Similarly, let $\mathrm{w} = \mathrm{w}_i^-$ be the solution of $\mathfrak{g}_i(\mathrm{w}) = \eta$, and then we obtain

$$\begin{aligned}
& \eta = \mathfrak{g}_\ell(\omega) < \mathfrak{g}_i(\mathfrak{w}_i^-) \;\; \Leftrightarrow \;\; \mathfrak{w}_i^- < \mathrm{w}_i^- \\
\Leftrightarrow \;\; & \mathfrak{f}_i(\mathfrak{w}_i^-) > \mathfrak{f}_i(\mathrm{w}_i^-) \;\;\;\;\;\; \Leftrightarrow \;\; \tau_\ell(\omega_o, \eta) > \tau_i(\omega_o, \eta),
\end{aligned}$$

where we noted that both $\mathfrak{f}_i$ and $\mathfrak{g}_i$ are strictly decreasing on L. Thus, (44) has been proved. ∎

Proof of Theorem 1: The developments from Lemma 1, leading to Theorem 1, have shown that Procedure 1 uniquely determines the controller (μ, ω_o, g, h) from $(\omega_o, \eta) \in \mathbb{F}_\ell$, as well as a solution $(\omega, \xi_\ell, \hat{\alpha})$ to the MHB equation (10). Moreover, the definition of $\mathbb{S}_\ell$ and Lemma 4 guarantee that it is a stable solution. Finally, the bounds in (23) and (24) follow from $0 < \mathfrak{f}_\ell(\omega) < 1$, which can be shown by a method similar to the proof of Theorem 2 in [12]. ∎

Proof of Lemma 3: Condition $A(\jmath\omega)\xi_\ell = 0$ in (10) can be written as

$$\begin{aligned}
& B\hat{u} = M(\omega)\xi_\ell, \\
& \hat{u} := R(\jmath\omega)\hat{y}, \quad M(\omega) := K - \omega^2 J + \jmath\omega D.
\end{aligned} \tag{45}$$

If B has full column rank, this condition holds if and only if

$$(I - BB^\dagger)M(\omega)\xi_\ell = 0, \quad \hat{u} = B^\dagger M(\omega)\xi_\ell. \tag{46}$$

If B does not have full column rank, (46) is only sufficient for (45), with the first condition in (46) remaining necessary. Using $J\xi_\ell = K\xi_\ell/\omega_\ell^2$, the real and imaginary parts of the first condition in (46) can be shown to be equivalent to (26) and (27), respectively. Using the definitions of $k_{\ell i}$ and $d_{\ell i}$ in (25), it can be verified that the second condition in (46) reduces equivalently to

$$\hat{u}_i = k_{\ell i}\sigma_{\ell i}(\omega)\hat{y}_i, \quad \sigma_{\ell i}(\omega) := 2(\omega/\omega_\ell)(\jmath\zeta_{\ell i} - \varpi_\ell).$$

On the other hand, the definition of $\hat{u}$ in (45) gives $\hat{u}_i = r_i(\jmath\omega)\hat{y}_i$, and we thus arrive at $r_i(\jmath\omega) = k_{\ell i}\sigma_{\ell i}(\omega)$. The rest of the proof is similar to that of Lemma 1. ∎

Proof of Theorem 2: Since the controller (μ, ω_o, g, h) is designed by Procedure 2, $(\omega, \xi_\ell, \hat{\alpha})$ is a solution of the MHB equation (10), and is uniquely determined. Furthermore, since $(\omega_o, \eta) \in \mathbb{S}_\ell$, the solution is a stable solution. The closeness of ω to either ω_ℓ or ω_o can also be shown as in the proof of Theorem 2 in [12]. ∎

Proof of Theorem 3: The closed-loop system (4) can be viewed as a feedback connection of a linear system $q = T(s)v$ and the nonlinearity $v = \psi I(q)$, where

$$T(s) := b(s)(M - HP(s)G), \quad P(s) := C(Js^2 + Ds + K)^{-1}B.$$

The system $T(s)$ is stable because the neuronal dynamics $b(s)$ and mechanical system $P(s)$ are both stable. The input v to $T(s)$ is bounded because $\psi \in \Psi$, and hence all the trajectories of the closed-loop system are bounded. By Theorem 1 in [41], boundedness of trajectories and hyperbolic instability of every equilibrium imply that the system is Y-oscillatory. On the other hand, the origin of (4) is the unique equilibrium due to $\psi(0) = 0$ and $b(0) = 0$, and is hyperbolic by supposition. Hence, it suffices to show instability of the origin. Below, we will show, using Lemma 5, that the origin is unstable whenever $(\omega_o, \eta) \in \mathbb{F}_\ell$.

Let us prove the statement by contraposition. Suppose the origin is not unstable. Then, by Lemma 5, condition (40) holds for all $i \in \mathbb{I}_n$. Consider the case where $\omega_o < \omega_\ell$. According to Lemma A.4 in [12], we have $\zeta_\ell\varpi = \mathfrak{g}_\ell(\omega_\ell) < \mathfrak{g}_\ell(\mathfrak{w}_\ell^+)$ because $\mathfrak{f}_\ell(\mathfrak{w}_\ell^+) = -\gamma_\ell \geq -\beta_\ell$. Since $\mathfrak{w}_\ell^- < \omega_o$, we have $\mathfrak{g}_\ell(\mathfrak{w}_\ell^-) < 0$. Therefore, we obtain

$$\zeta_\ell\varpi_o < \mathfrak{g}_\ell(\mathfrak{w}_\ell^+) \leq \eta \leq g_\ell(\mathfrak{w}_\ell^-) < 0,$$

which violates $(\omega_o, \eta) \in \mathbb{F}_\ell$. In the case of $\omega_o > \omega_\ell$, by a similar argument, we obtain

$$0 < \mathfrak{g}_\ell(\mathfrak{w}_\ell^+) \leq \eta \leq g_\ell(\mathfrak{w}_\ell^-) < \zeta_\ell\varpi_o.$$

Thus we have $(\omega_o, \eta) \notin \mathbb{F}_\ell$ again. We have now proved that (ω_o, η) does not belong to $\mathbb{F}_\ell$ if the origin is not unstable. ∎

REFERENCES

[1] K. G. Holt, J. Hamill, and R. O. Andres, "Predicting the minimal energy costs of human walking," *Medicine and Science in Sports and Exercise*, vol. 23, no. 4, pp. 491–498, 1991.

[2] F. Delcomyn, "Neural basis of rhythmic behavior in animals," *Science*, vol. 210, 1980.

[3] S. Grillner, J. T. Buchanan, P. Walker, and L. Brodin, *Neuronal Control of Rhythmic Movements in Vertebrates*. New York: Wiley, 1988.

[4] G. N. Orlovsky, T. G. Deliagina, and S. Grillner, *Neuronal Control of Locomotion: From Mollusc to Man*. Oxford University Press, 1999.

[5] W. B. K. Jr., R. Calabrese, and W. O. Friesen, "Neuronal control of leech behavior," *Prog. in Neurobiol.*, vol. 76, pp. 279–327, 2005.

[6] A. H. Cohen, G. B. Ermentrout, T. Kiemel, N. Kopell, K. A. Sigvardt, and T. L. Williams, "Modeling of intersegmental coordination in the lamprey central pattern generator for locomotion," *Trends. in Neurosci.*, vol. 15, no. 11, pp. 434–438, 1992.

[7] X. Yu, B. Nguyen, and W. O. Friesen, "Sensory feedback can coordinate the swimming activity of the leech," *J. Neurosci.*, vol. 19, no. 11, pp. 4634–4643, 1999.

[8] T. Iwasaki and M. Zheng, "Sensory feedback mechanism underlying entrainment of central patter generator to mechanical resonance," *Biological Cybernetics*, vol. 94, no. 4, pp. 245–261, 2006.

[9] B. W. Verdaasdonk, H. F. Koopman, and F. C. van der Helm, "Energy efficient and robust rhythmic limb movement by central pattern generators," *Neural Network*, vol. 19, no. 4, pp. 388–400, 2006.

[10] ——, "Resonance tuning in a neuro-musculo-skeletal model of the forearm," *Biological Cybernetics*, vol. 96, no. 2, pp. 165–180, 2007.

[11] C. A. Williams and S. P. DeWeerth, "A comparison of resonance tuning with positive versus negative sensory feedback," *Biological Cybernetics*, vol. 96, no. 6, pp. 603–614, 2007.

[12] Y. Futakata and T. Iwasaki, "Formal analysis of resonance entrainment by central patter generator," *J. Math. Biol.*, vol. 57, no. 2, pp. 183–207, 2008.

[13] T. Glad and L. Ljung, *Control Theory – Multivariable and Nonlinear Methods*. Taylor & Francis, 2000.

[14] H. K. Khalil, *Nonlinear Systems*, 2nd ed. Prentice Hall, 1996.

[15] D. A. Linkens, "Analytical solution of large numbers of mutually coupled nearly sinusoidal oscillators," *IEEE Trans. Circ. Sys.*, vol. 21, no. 2, pp. 294–300, 1974.

[16] A. Collado, F. Ramirez, and J. P. Pascual, "Harmonic-balance analysis and synthesis of coupled-oscillator arrays," *IEEE Microwave and Wireless Components Letters*, vol. 14, no. 5, pp. 192–194, 2004.

[17] D. W. Berns, J. L. Moiola, and G. Chen, "Feedback control of limit cycle amplitudes from a frequency domain approach," *Automatica*, vol. 34, no. 12, pp. 1567–1573, 1998.

[18] A. Tesi, E. H. Abed, R. Genesio, and H. O. Wang, "Harmonic balance analysis of period-doubling bifurcations with implications for control of nonlinear dynamics," *Automatica*, vol. 32, no. 9, pp. 1255–1271, 1996.

[19] T. G. Brown, "The intrinsic factors in the act of progression in the mammal," *Proc. Roy. Soc. Lond.*, vol. 84, pp. 308–319, 1911.

[20] W. O. Friesen, "Reciprocal inhibition: A mechanism underlying oscillatory animal movements," *Neurosci. and Biobehav. Rev.*, vol. 18, no. 4, pp. 547–553, 1994.

[21] T. Iwasaki, "Multivariable harmonic balance for central patter generators," *Automatica*, vol. 44, no. 12, pp. 4061–4069, 2008.

[22] Z. Chen, M. Zheng, W. O. Friesen, and T. Iwasaki, "Multivariable harmonic balance analysis of neuronal oscillator for leech swimming," *J. Computational Neuroscience*, vol. 25, no. 3, pp. 583–606, 2008.

[23] Z. Chen and T. Iwasaki, "Matrix perturbation analysis for weakly coupled oscillators," *Sys. Contr. Lett.*, vol. 58, no. 2, pp. 148–154, 2009.

[24] ——, "Circulant synthesis of central pattern generators with application to control of rectifier systems," *IEEE Trans. Automat. Contr.*, vol. 53, no. 3, pp. 273–286, 2008.

[25] V. A. Yakubovich, "Frequency-domain criteria for oscillation in nonlinear systems with one stationary nonlinear component," *Siberian Mathematical Journal*, vol. 14, no. 5, pp. 768–788, 1973.

[26] Y. Futakata and T. Iwasaki, "Entrainment of central pattern generators to neuronal oscillations of collocated mechanical systems," in *IEEE Conf. Decision and Contr.*, Cancun, Mexico, Dec. 2008, pp. 5220–5225.

[27] K. Matsuoka, "Sustained oscillations generated by mutually inhibiting neurons with adaptation," *Biol. Cybern.*, vol. 52, pp. 367–376, 1985.

[28] J. Cang, X. Yu, and W. O. Friesen, "Sensory modification of leech swimming: interactions between ventral stretch receptors and swim-related neurons," *J. Comp. Physiol.. A*, vol. 187, pp. 569–579, 2001.

[29] P. D. Brodfuehrer, E. A. Debski, B. A. O'Gara, and W. O. Friesen, "Neuronal control of leech swimming," *J. Neurobiology*, vol. 27, no. 3, pp. 403–418, 1995.

[30] Y. Futakata, "Natural mode entrainment by CPG-based decentralized feedback controllers," Ph.D. Dissertation, Mechanical and Aerospace Engineering, University of Virginia, Aug. 2009.

[31] J. Guckenheimer and P. Holmes, *Nonlinear Oscillations, Dynamical Systems, and Bifurcations of Vector Fields*. Springer-Verlag, 1983.

[32] M. Farkas, *Periodic Motions*. Springer-Verlag, 1994.

[33] J. Marsden and M. McCracken, *The Hopf bifurcation and its applications*. New York: Springer-Verlag, 1976.

[34] I.I. Blechman. *Synchronization of dynamical systems*. Science, 1971.

[35] G. B. Ermentrout and N. Kopell, "Frequency plateaus in a chain of weakly coupled oscillators, i," *SIAM J. Math. Anal.*, vol. 15, no. 2, pp. 215–237, march 1984.

[36] E. M. Izhikevich, *Dynamical Systems in Neuroscience: The Geometry of Excitability and Bursting*. Cambridge, MA: The MIT Press, 2006.

[37] U. T. Jonsson, C. Y. Kao, and A. Megretski, "Robustness of periodic trajectories," *IEEE Trans. Automat. Contr.*, vol. 47, no. 11, pp. 1842–1856, 2002.

[38] W. Lohmiller and J. J. E. Slotine, "On contraction analysis for non-linear systems," *Automatica*, vol. 34, no. 6, pp. 683–696, 1998.

[39] Q. C. Pham and J. J. Slotine, "Stable concurrent synchronization in dynamic system networks," *Neural Networks*, vol. 20, pp. 62–77, 2007.

[40] T. Bliss, T. Iwasaki, and H. Bart-Smith, "CPG control of a tensegrity morphing structure for biomimetic applications," *Advances in Science and Technology*, vol. 58, pp. 137–142, 2008.

[41] A. Pogromsky, T. Glad, and H. Nijmeijer, "On diffusion driven oscillations in coupled dynamical systems," *Int. J. Bifurcation and Chaos*, vol. 9, no. 4, pp. 629–644, 1999.

[42] A. Pogromsky and H. Nijmeijer, "Cooperative oscillatory behavior of mutually coupled dynamical systems," *IEEE Trans. Circuit and Systems – I: Fundamental Theory and Applications*, vol. 48, no. 2, pp. 152–162, 2001.

[43] D. Efimov and A. Fradkov, "Oscillation conditions of nonlinear systems with static feedback," *Automation and Remote Control*, vol. 66, no. 2, pp. 249–264, 2005.

[44] A. Mees, *Dynamics of Feedback Systems*. John Wiley & Sons, 1981.

[45] J. Blair and T. Iwasaki, "Optimal gaits for mechanical rectifier systems," *IEEE Trans. Auto. Contr.*, 2010, (To appear).

Yoshiaki Futakata received the B.E. and M.S. degrees from Tokyo Institute of Technology, Japan in 1999 and 2001 respectively, and his Ph.D. degree in Mechanical and Aerospace Engineering from University of Virginia in 2009.

Dr. Futakata is currently a postdoctoral fellow in Information Physics and Computing at the University of Tokyo, and his current research interest is to understand mechanisms for synchronization of coupled nonlinear oscillators with various coupling structures.

Tetsuya Iwasaki received his B.S. and M.S. degrees in Electrical and Electronic Engineering from the Tokyo Institute of Technology (Tokyo Tech) in 1987 and 1990, respectively, and his Ph.D. degree in Aeronautics and Astronautics from Purdue University in 1993. He held a Post-Doctoral Research Associate position at Purdue University (1994-1995), and faculty positions at Tokyo Tech (1995-2000) and at the University of Virginia (2000-2009), before joining the UCLA faculty as Professor of Mechanical and Aerospace Engineering.

Dr. Iwasaki's current research interests include biological control mechanisms underlying animal locomotion, nonlinear oscillators, and robust/optimal control theories and their applications to engineering systems. He has received CAREER Award from NSF, Pioneer Prize from SICE, George S. Axelby Outstanding Paper Award from IEEE, Rudolf Kalman Best Paper Award from ASME, and Best Biomedical/Biosystem Paper Award at the 8th World Congress on Intelligent Control and Automation. He has served as associate editor of *IEEE Transactions on Automatic Control*, *Systems & Control Letters*, *IFAC Automatica*, and *International Journal of Robust and Nonlinear Control*. He is a Fellow of IEEE.